Digital Communications and Networks 10 (2024) 481–497

Contents lists available at ScienceDirect

Digital Communications and Networks

journal homepage: www.keaipublishing.com/dcan

A CSMA/CA based MAC protocol for hybrid Power-line/Visible-light communication networks: Design and analysis

Sheng Hao [a,b,*], Huyin Zhang [c], Fei Yang [c], Chenghao Li [d], Jing Wang [e]

[a] School of Computer Science, Central China Normal University, Wuhan, 430079, PR China
[b] Hubei Key Laboratory of intelligent Robot (Wuhan Institute of Technology), Wuhan, 430079, PR China
[c] School of Computer Science, Wuhan University, Wuhan, 430079, China
[d] School of Information Science and Engineering, Shandong Normal University, Jinan, 250000, China
[e] School of Computer Science, Hubei University of Technology, Wuhan, 430079, China

ARTICLE INFO

Keywords:
Hybrid power-line/Visible light communication (HPVC) networks
MAC protocol
CSMA/CA
IEEE 802.15.7
IEEE 1901
Performance analysis

ABSTRACT

Hybrid Power-line/Visible-light Communication (HPVC) network has been one of the most promising Cooperative Communication (CC) technologies for constructing Smart Home due to its superior communication reliability and hardware efficiency. Current research on HPVC networks focuses on the performance analysis and optimization of the Physical (PHY) layer, where the Power Line Communication (PLC) component only serves as the backbone to provide power to light Emitting Diode (LED) devices. So designing a Media Access Control (MAC) protocol remains a great challenge because it allows both PLC and Visible Light Communication (VLC) components to operate data transmission, i.e., to achieve a true HPVC network CC. To solve this problem, we propose a new HPC network MAC protocol (HPVC MAC) based on Carrier Sense Multiple Access/Collision Avoidance (CSMA/CA) by combining IEEE 802.15.7 and IEEE 1901 standards. Firstly, we add an Additional Assistance (AA) layer to provide the channel selection strategies for sensor stations, so that they can complete data transmission on the selected channel via the specified CSMA/CA mechanism, respectively. Based on this, we give a detailed working principle of the HPVC MAC, followed by the construction of a joint analytical model for mathematical-mathematical validation of the HPVC MAC. In the modeling process, the impacts of PHY layer settings (including channel fading types and additive noise feature), CSMA/CA mechanisms of 802.15.7 and 1901, and practical configurations (such as traffic rate, transit buffer size) are comprehensively taken into consideration. Moreover, we prove the proposed analytical model has the solvability. Finally, through extensive simulations, we characterize the HPVC MAC performance under different system parameters and verify the correctness of the corresponding analytical model with an average error rate of 4.62% between the simulation and analytical results.

1. Introduction

Internet of things (IoT) has been a popular technology that connects together all the physical entities embedded with sensors and different type network systems to realize the efficient communication target [1,2]. The concept of IoT also pushes forward worldwide efforts to design a new generation of effective, reliable, flexible, and low-energy consumption telecommunication technology [3,4]. In recent years, Hybrid Communication (HC) IoT systems have received increasing attention in order to improve the reliability and coverage of telecommunication infrastructures in both indoor and outdoor environments [5–7]. Particularly, hybrid Power-line/Visible-light communication (HPVC) networks [8–17] are increasingly employed for transmitting status information or sensor data in Smart Home/Grid and Industrial IoT (IIoT), since it can combine dual-medium, integrate superior communication capabilities and resources, improve the system performance and security. Conventional HPVC networks generally use the Power-Line Communication (PLC) component as the backbone to supply power for Visible-Light Communication (VLC) component [13,14]. However, with the breakthrough of PLC technology, PLC devices can achieve highly efficient data rates reaching up to 1.5 Gbps [18,19]. Hence, with the exception of using VLC component, how to use the PLC component to accomplish the data transmission should be taken into consideration for HPVC networks. Recently, some HC IoT devices have acquired the capability of

* Corresponding author. School of Computer Science, Central China Normal University, Wuhan, 430079, PR China.
E-mail addresses: 809023460@qq.com, mikeshao@ccnu.edu.cn (S. Hao), 2008301500139@whu.edu.cn (H. Zhang), young-fly@whu.edu.cn (F. Yang), greatlch@126.com (C. Li), 36483799@qq.com (J. Wang).

https://doi.org/10.1016/j.dcan.2022.09.019
Received 23 July 2021; Received in revised form 1 September 2022; Accepted 23 September 2022
Available online 1 October 2022

simultaneously utilizing multi-type channels (such as employing VLC&WLC (Wireless Communication) channels, or WLC&PLC channels, or VLC&PLC channels) to finish data delivery tasks [6,20–26].

1.1. Motivations

Current research on HPVC networks [8–17,24–26] has focused on Bit-Error-Rate (BER) measurements, power allocation optimization, and Multiple-Input Multiple-Output (MIMO) based capacity enhancement. All these works are proposed around the Physical (PHY) layer of HPVC networks, where PLC component is only regarded as the power source to support VLC component, namely the PLC and VLC components follow a cascaded mode. Therefore, it's a challenging work to design a reasonable MAC protocol for HPVC networks, which can utilize the existing standards of PLC and VLC (IEEE 1901 [27] and IEEE 802.15.7 [28]), and allow the sensor stations of HPVC networks to operate data transmission with a "parallel mode" (i.e., using VLC and PLC mediums to accomplish the communication simultaneously). In the meantime, it's also significant to establish a rigorous analytical model to supply the theory support for the MAC protocol.

From the viewpoint of practical engineering, the VLC technology employing Light Emitting Diodes (LEDs) has become a popular option for high speed communication purposes due to its multiple advantages including green communication, high security, efficient capacity transmission, ready availability and easy deployment [8–14]. Because of this, VLC is growing as a potential candidate for providing wireless network access to IoT devices. Furthermore, PLC technology has been a great commercial success and has proven to be a robust and cost-optimized communication mechanism that is expected to benefit more than 30% of the global population by 2022 [29–31]. The power lines of PLCs can be easily connected to LED-equipped sensor stations and can also serve as their transmission medium [8,11], so the convergence of PLCs and VLCs, i.e., HPVC networks, is bound to be a technology for high data rates and reliable transmission. Along with this, HPVC networks have many potential superiorities such as safety communication, easy and economical deployment and power efficient transmission. Existing HPVC-based IoT applications have related to diverse domains including Smart Grid/-Home, intelligent street lamp, telemedicine systems, Intelligent Mining, photovoltaic system and Industry 4.0, so the proposed MAC protocol is beneficial for us to manage HPVC network efficiently and has practical value to guide the construction of HC IoT system.

1.2. Contributions

The core contributions of the paper are as follows:

- On the basis of integrating the IEEE 802.15.7 standard of VLC and the IEEE 1901 standard of PLC, a CSMA/CA-based HPVC network MAC protocol is proposed (referred to as HPVC MAC). First, an Additional Assistance (AA) layer is added between the MAC layer and the PHY layer to help sensor stations select the appropriate channel. The AA layer sets up three Channel Selection (CS) strategies: Random Assignment (RA), Traffic Awareness (TA), and Channel Awareness (CA), meaning that if sensor stations have packets and need to transmit them to a Coordination Point (CP) station, they will use one of the three CS strategies. After confirming the channel type (PLC or VLC), sensor stations begin to execute the corresponding CSMA/CA mechanism to compete for the specified medium (if selecting VLC channel, they carry out IEEE 802.15.7 protocol; otherwise IEEE 1901 protocol), and for the senor stations having occupied PLC or VLC channel, they would transmit data packets to the CP station.[1] The other sensor stations that do not occupy PLC and VLC channels enter the idle state.
- To mathematically analyze the proposed HPVC MAC protocol, a joint analytical model is established. In the modeling process, we firstly build the PHY layer model to reflect the impacts of channel fading types (containing PLC and VLC channels) and impulsive noise of PLC on data transmission. Then a "Double-Folding" Heterogeneous Discrete Markov Chain (DFH DMC) model is constructed to depict the CSMA/CA process of HPVC MAC, where the influence of transit buffer size, traffic rate, Quality of Information (QoI) [32,33] and CS strategies are comprehensively considered. Through utilizing the above two models, we derive the closed-form expressions of system metrics of HPVC MAC protocol, including the Goodput, average MAC service time, overflow probability, expected QoI, average queue length and etc.
- It is demonstrated that the proposed joint analysis model is solvable and has an upper bound performance on the expected QoI of one successful transmission.
- A large number of simulation experiments are carried out to characterize the performance of the HPVC MAC protocol and verify the correctness of the corresponding analysis model.

1.3. Paper outline

The rest of our paper is organized as follows. Related works are reviewed in Section 2. Overview of IEEE 802.15.7 and 1901 is given in Section 3. The working principle of HPVC MAC protocol, joint analytical model and solvability analysis are presented in Section 4. Simulation and evaluation results are discussed in Section 5. Finally, we conclude our work in Section 6.

2. Related work

2.1. Studies of HPVC networks

Current studies for HPVC networks mainly focused on the PHY layer performance evaluation and optimization [8–17,24–26]. Typically, Kumar et al. proposed an analytical model to evaluate the BER performance of HPVC networks, where Orthogonal Frequency Division Multiplexing (OFDM) technique was considered in the modeling process [8]. In Ref. [9], Kashef et al. investigated HPVC networks with Radio Frequency (RF) relay, and developed an analytical model to allocate the transmission power to maximize the achievable rate. In Refs. [11–14], the authors analyze the PHY layer performance of HPVC networks in an indoor environment, where the effects of multiple users in the downlink [11], multiple access techniques [12], mobility characteristics [13], and hybrid collaboration strategies [14] are considered, respectively. In Ref. [15], Gheth et al. evaluated the performance of cascaded indoor HPVC system with an Amplify-and-Forward (AF) relay, and verified that the AF relay has a positive effect on the performance of HPVC systems. In Refs. [16,17], the authors demonstrated the Non Orthogonal Multiple Access (NOMA) scheme can achieve better performance in system capacity and power saving, and designed a NOMA scheme-based power allocation strategy for HPVC networks. Furthermore, Khalid et al. examined how to use both PLC and VLC channels to accomplish the data transmission for HPVC networks [26]. This work provided the important basis of simultaneously using multiple channels to transmit data packets in HPVC networks (i.e., designing the HPVC MAC protocol is technically feasible). Although the above mentioned works can help us comprehend HPVC networks more deeply, they only studied the PHY layer of HPVC networks. Therefore, proposing a reasonable MAC protocol for HPVC networks would be quite a different and challenging work.

[1] It's possible in our MAC protocol that two sensor stations that respectively occupy PLC and VLC channels in the same time slot.

2.2. Studies of IEEE 1901 and IEEE 802.15.7 analysis

Existing analytical studies of IEEE 1901 and 802.15.7 protocols can help us build the analytical model of the proposed MAC protocol. In Ref. [34], a semi-Markov based analytical model was proposed to depict the CSMA/CA mechanism of saturated 1901 protocol. Next, Vlachou et al. made a series of analysis for 1901 protocol using Renewal theory and strong law of large number (SLLN) [35–39], and they can be summarized as four parts: (1) establishing the basic analytical model and proving it has real number solutions [35,36]; (2) revealing the relationship between delay and throughput [37]; (3) improving the MAC performance of 1901 (according to their basic analytical model) [38]; (4) investigating the stability feature of 1901 protocol [39]. It should be pointed out that Vlachou's works are valid only for saturated conditions. Similarly, Cano et al. used renewal process theorem to build a theoretical model for IEEE 1901 protocol in saturated conditions [40]. In Ref. [41], Hao et al. provided a unified theoretical framework for the 1901 protocol that can be used in both homogeneous and heterogeneous environments, and then they further constructed a theoretical model of the 1901 protocol for multi-hop PLC networks [42].

For IEEE 802.15.7 analysis, Le et al. proposed a basic model to investigate the MAC performance of saturated VLC networks considering the impact of relay node's cooperative transmission [43]. Musa et al. constructed a discrete Markov chain to analyze the CSMA/CA mechanism of 802.15.7, where the behavior of Contention Period Access (CAP) is taken into consideration [44]. In Ref. [45], Nobar et al. proposed a Markov chain model to examine the time slot random access mechanism of the 802.15.7 protocol under saturation conditions, and compared to previous studies [43,44], the effects of frame length and packet length were analyzed in the modeling process. Through further extending this model (combining with queueing theory), the authors studied the performance of 802.15.7 with unsaturated traffic [46]. In addition, Dang et al. established a comprehensive model to thoroughly analyze the MAC performance of 802.15.7, in which a retransmission policy is added at MAC layer [47].

Clearly, the above mentioned analytical models are valid only for single type MAC protocol (IEEE 1901 or 802.15.7), which cannot be directly employed to analyze the proposed MAC protocol for HPVC networks.

3. Overview of IEEE 802.15.7 and IEEE 1901 standards

3.1. IEEE 802.15.7 standard

IEEE 802.15.7 standard uses a CSMA/CA process to compete for the VLC medium [28]. When a data packet arrives at the sensor station, it sets the values of backoff stages BS and backoff exponent BE (the initial value of BS is 1). If the sensor station tries to transmit its data packet, it enters into the initial BS, and waits for a random number of time slots (one time slot is defined as unit backoff period, UBP) between $[1, W_{BS}](W_{BS} = 2^{BE})$. As the waiting time slots exhaust, the CCA (clear channel assignment) mechanism [28] is enabled. After waiting a time duration (determined by CCA), the sensor station attempts to transmit the data packet. If the channel is sensed to be idle, the packet would be transmitted; Otherwise, the sensor station adjusts the values of BE and BS, i.e.,

$$\begin{cases} BE = \min\{BE + 1, BE_{\max}\} \\ BS = \min\{BS + 1, l\} \end{cases} \tag{1}$$

where $BE_{\max}$ denotes the maximum value of backoff exponent, l denotes the maximum value of backoff stage.

3.2. IEEE 1901 standard

IEEE 1901 standard employs a backoff counter along with a deferral counter. The backoff counter process (BCP) of 1901 is similar to that of 802.11 (referring to Refs. [27,31] for the detailed description). The Deferral Counter Process (DCP) of 1901 operates as following: when the sensor station enters backoff stage k, it sets the initial deferral counter as d_k (the values of d_k are shown in Table 1), and when it senses that the PLC medium busy, the sensor station decreases d_k by 1 (executing the BCP at the same time); if the deferral counter reaches to 0 and the medium is sensed busy (i.e., sensing the medium busy $d_k + 1$ times), it would enter the next backoff stage $k + 1$ (if already at the last backoff stage m, it re-enters this stage).

Moreover, 1901 has only four backoff stages (i.e., $m = 4$), and defines four priority classes ($CA0 - CA3$), in which $CA0/CA1$ (or $CA2/CA3$) constitutes one priority type. Note that the change rule of the backoff counter size Q_k depends on the corresponding priority type (the values of Q_k are shown in Table 1).

4. System model

In this part, we firstly provide the working principle of HPVC MAC protocol, then construct the corresponding analytical model, and finally demonstrate the proposed analytical model has the solvability.

4.1. The detailed working principle of HPVC MAC protocol

Before designing the HPVC MAC protocol, we assume the HPVC network adopts a star-shaped, convergent topology [39,48], and it is composed of N sensor stations and one CP station. Each station equips with a LED device, that can be used to accomplish the transmission with VLC pattern. At the same time, sensor stations are connected to the CP station through power line, so that they can select PLC pattern to transmit data packets (the overall network scene is shown as Fig. 1).

The execution process of HPVC MAC protocol is divided into two steps. Firstly, to efficiently utilize multiple channels of the HPVC network, we choose one CS strategy at the AA layer to help sensor stations determine the access channel (noting a sensor station cannot use both channels to transmit one packet in the meantime). Here we set three different CS strategies, i.e., RA, TA and CA, and they operate as follows:

At the beginning, the sensor station checks its transit buffer. Only if the sensor station has packet and needs to transmit, it intends to find a channel (PLC or VLC) for its transmission. The time duration of CS is defined as Δ.

(1) **RA CS**: The sensor station randomly selects one of the two channels for transmitting data regardless of its traffic or channel status. Thus, the probability of selecting PLC (or VLC) channel as the access medium P_{PLC} (or P_{VLC}) equals to 0.5 ($P_{VLC} = 1 - P_{PLC}$).
(2) **TA CS**: If the sensor station's current traffic rate is smaller than the denoted threshold value λ_{th}, VLC channel is chosen for data transmissions; otherwise PLC channel is employed. Assuming that

Table 1
The backoff counter size (Q_k) and initial deferral counter (d_k) of IEEE 1901 standard [27].

Priority class:	*CA0*	*CA1*	*CA2*	*CA3*
backoff stage k	Q_k	d_k	Q_k	d_k
1	8	0	8	0
2	16	1	16	1
3	32	3	16	3
4	64	15	32	15

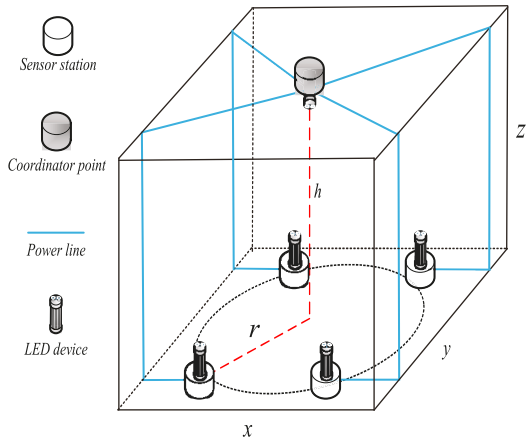

Fig. 1. The indoor scenario of HPVC system.

the packet generation process of a sensor station follows Poisson distribution with an average rate λ, the probability of selecting PLC (or VLC) channel as the access medium P_{PLC} (or P_{VLC}) can be represented as

$$\begin{cases} P_{V\,LC} = \sum_{i=0}^{\lambda_{th}} \dfrac{\lambda^i \cdot exp(-\lambda)}{i!} \\ P_{PLC} = 1 - P_{V\,LC} = 1 - \sum_{i=0}^{\lambda_{th}} \dfrac{\lambda^i \cdot exp(-\lambda)}{i!} \end{cases} \tag{2}$$

(3) **CA CS**: The sensor station selects a channel based on the comparison of outage probability (i.e., the probability that the packet is received in outage [13,29]). Let ζ_p (or ζ_v) be the required minimum SNR (signal to noise ratio) of PLC (or VLC) channel for successfully accepting a data packet, the outage probabilities of PLC and VLC channels (P_{out}^{PLC} and $P_{out}^{V\,LC}$) can be respectively given as

$$\begin{cases} P_{out}^{PLC} = Prb\{SNR_{PLC} < \zeta_p\} \\ P_{out}^{V\,LC} = Prb\{SNR_{V\,LC} < \zeta_v\} \end{cases} \tag{3}$$

where $Prb\{\ell\}$ denotes the probability that case ℓ is true.

Thus, P_{PLC} and P_{VLC} are developed as

$$\begin{cases} P_{PLC} = \dfrac{1 - P_{out}^{PLC}}{2 - P_{out}^{PLC} - P_{out}^{VLC}} \\ P_{V\,LC} = 1 - P_{PLC} = \dfrac{1 - P_{out}^{PVC}}{2 - P_{out}^{PLC} - P_{out}^{VLC}} \end{cases} \tag{4}$$

Remark 1. The expansion forms of P_{out}^{PLC} and $P_{out}^{V\,LC}$ are shown in the following subsection.

After choosing the appropriate channel, the sensor stations would initialize corresponding CSMA/CA mechanism (IEEE 1901 standard or IEEE 802.15.7 standard) to compete for this designated channel. Once a sensor station occupies the specified channel (PLC or VLC), it can transmit its packet. If the packet is successfully delivered or dropped due to the limitation of maximum *BS* (only occurring at 802.15.7 [47]), the sensor station would reset to the beginning state and stars a new cycle by executing a type of CS strategy. The operation and corresponding flow chart of HPVC MAC are reported in Procedure 1 and Fig. 2 (see the top of next page), respectively.

Procedure 1: Operation of HPVC MAC protocol

1: **For** each sensor station
2: Uses the CS strategy to choose an appropriate channel (PLC or VLC channel);
3: **If** the sensor station chooses the PLC channel;
4: Executes the CSMA/CA process of IEEE 1901 protocol (please see Section 3 and [27]) to occupy the PLC channel;
5: **Else** (choosing the VLC channel);
6: Executes the CSMA/CA process of IEEE 802.15.7 protocol (please see Section 3 and [28]) to occupy the VLC channel;
7: **If** the sensor station successfully occupies the selected channel;
8: Deliveries the data packet to CP station;
9: **Else**
10: Senses the channel state and continues to execute the corresponding CSMA/CA process.
9: **End If**
10: **End if**
11: **End For**

4.2. Joint analytical model of HPVC MAC protocol

In this part, a joint analytical model will be established to mathematically analyze the performance of HPVC MAC protocol from a cross-layer perspective. The detailed modeling process is divided into three steps: (1) Constructing the PHY layer model to reflect the impacts of channel fading type (containing PLC and VLC channels) and additive noise of PLC on HPVC MAC; (2) Building the MAC layer model to depict the CSMA/CA process of HPVC MAC; (3) Deriving the closed-form expressions of system metrics for HPVC MAC.

4.2.1. PHY layer model

4.2.1.1. PLC channel model. The PLC component generally employs a Log-normal fading channel [49],[2] thus the PDF (probability density function) of PLC channel gain $f_P(h_P)$ is written as

$$f_P(h_P) = \frac{1}{\sqrt{2\pi\sigma_P^2} \cdot h_P} \cdot exp\left(- \frac{(\ln(h_P) - \mu_P)^2}{2\sigma_P^2} \right), h_P > 0 \tag{5}$$

where h_P denotes the channel gain of PLC channel, σ_P and μ_P the scale parameters of Log-normal distribution.

Since the noise of PLC channel z_P contains background noise and potentially impulsive noise [49], we have

$$z_P = N_I \cdot n_p + N_B \tag{6}$$

where N_I is the impulsive noise sample, N_B the background noise sample, and n_p the Poisson arrival process of impulsive noise in PLC channel [49]. Here N_I and N_B are regarded as additive white Gaussian noises, i.e., $N_I \sim \mathcal{N}(0, \sigma_I^2)$ and $N_B \sim \mathcal{N}(0, \sigma_B^2)$ [13] (σ_I^2 and σ_B^2 represent the noise variances).

Hence, the PDF $f_z(.)$ of z_P can be represented as

$$\begin{aligned} f_z(z_P) &= (1 - P_I) \cdot \mathcal{N}(0, \sigma_B^2) + P_I \cdot \mathcal{N}(0, \sigma_I^2 + \sigma_B^2) \\ &= P_I \cdot \left(\frac{1}{\sqrt{2\pi(\sigma_I^2)}} \cdot exp\left(- \frac{z_P^2}{2\sigma_I^2} \right) \right) + \\ &(1 - P_I) \cdot \left(\frac{1}{\sqrt{2\pi(\sigma_I^2 + \sigma_B^2)}} \cdot exp\left(- \frac{z_P^2}{2(\sigma_I^2 + \sigma_B^2)} \right) \right) \end{aligned} \tag{7}$$

[2] PLC channel can be also modeled as Rayleigh distribution [50].

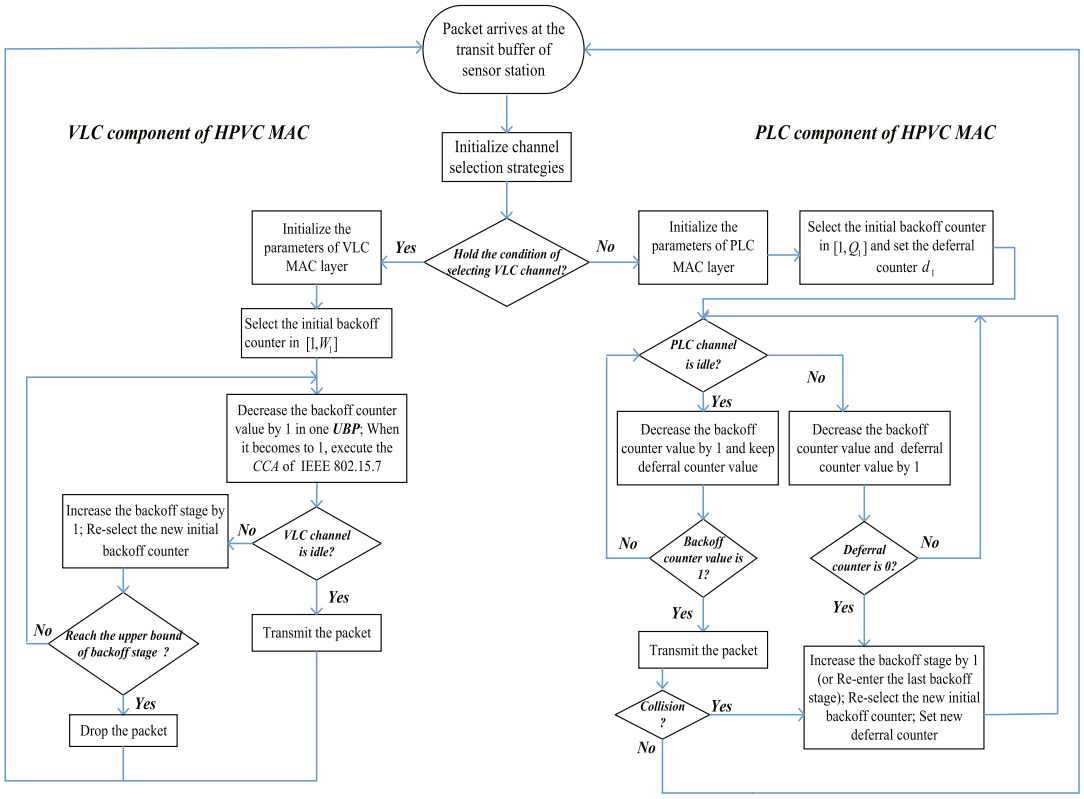

Fig. 2. Execution flow of HPVC MAC.

where $P_I = \rho \cdot T$ is the statistical occurrence probability of impulsive noise, ρ and T are the arrival rate and the duration of the occurrence of impulsive noise. Furthermore, $\sigma_I^2 = \beta \cdot \sigma_B^2$ (β is a positive integer).

Let γ_P be the SNR of PLC channel, E_p the transmission power in PLC channel, the instantaneous SNR of PLC channel γ_P is given by

$$\gamma_P = \begin{cases} \dfrac{E_p \cdot |h_P|^2}{\sigma_B^2} & w.p. \quad 1-\rho \cdot T \\ \dfrac{E_p \cdot |h_P|^2}{\sigma_B^2 + \sigma_I^2} & w.p. \quad \rho \cdot T \end{cases} \tag{8}$$

As a consequence, the PDF $f_\gamma(.)$ of γ_P is developed as

$$\begin{aligned} f_\gamma(\gamma_P) = (1-\rho\cdot T)\cdot \frac{1}{\sqrt{2\pi\sigma_{P'}^2\gamma_P}}\cdot exp\left(-\frac{\left(\ln\left(\frac{\gamma_P\cdot\sigma_B^2}{E_p}\right)-\mu_{P'}\right)^2}{2\sigma_{P'}^2}\right) \\ +\rho\cdot T\cdot \frac{1}{\sqrt{2\pi\sigma_{P'}^2\gamma_P}}\cdot exp\left(-\frac{\left(\ln\left(\frac{\gamma_P\cdot(\sigma_I^2+\sigma_B^2)}{E_p}\right)-\mu_{P'}\right)^2}{2\sigma_{P'}^2}\right) \end{aligned} \tag{9}$$

where $\sigma_{P'}^2$ and $\mu_{P'}$ are respectively written as

$$\begin{cases} \sigma_{P'}^2 = 4\sigma_P^2 \\ \mu_{P'} = 2\mu_P \end{cases} \tag{10}$$

Using moment matching method [48], we can further express Eq. (9) as ($\Gamma(.)$ is the Gamma function)

$$\begin{aligned} f_\gamma(\gamma_P) = (1-\rho\cdot T)\cdot\left(\frac{m_1}{\Omega_1}\right)^{m_1}\cdot\frac{\gamma_P^{m_1-1}}{\Gamma(m_1)}\cdot exp\left(-\frac{\Gamma(m_1)}{\Omega_1}\right)+ \\ \rho\cdot T\cdot\left(\frac{m_2}{\Omega_2}\right)^{m_2}\cdot\frac{\gamma_P^{m_2-1}}{\Gamma(m_2)}\cdot exp\left(-\frac{\Gamma(m_2)}{\Omega_2}\right) \end{aligned} \tag{11}$$

where m_1, m_2, Ω_1 and Ω_2 are denoted as

$$\begin{cases} m_1 = m_2 = [exp(\sigma_{P'}^2 - 1)]^{-1} \\ \Omega_1 = exp\left(\mu_{P'} + \ln\left(\dfrac{E_p}{\sigma_B^2}\right)\right)\cdot\sqrt{1+\dfrac{1}{m_1}} \\ \Omega_2 = exp\left(\mu_{P'} + \ln\left(\dfrac{E_p}{(\sigma_B^2+\sigma_I^2)}\right)\right)\cdot\sqrt{1+\dfrac{1}{m_2}} \end{cases} \tag{12}$$

Then, the CDF (cumulative distribution function) of SNR for PLC channel $F_\gamma(\gamma_P)$ is accordingly derived as

$$\begin{aligned} F_\gamma(\gamma_P) = \quad (1-\rho\cdot T)\cdot\left(\frac{1}{\Gamma(m_1)}\cdot\mathcal{G}_{1,2}^{1,1}\left[\frac{m_1\gamma_P}{\Omega_1}\Big|_{m_1,0}^{1}\right]\right)+ \\ \rho\cdot T\cdot\left(\frac{1}{\Gamma(m_2)}\cdot\mathcal{G}_{1,2}^{1,1}\left[\frac{m_2\gamma_P}{\Omega_2}\Big|_{m_2,0}^{1}\right]\right) \end{aligned} \tag{13}$$

where $\mathcal{G}_{x_3,x_4}^{x_1,x_2}[y|_{b_1,\ldots,b_{x_4}}^{a_1,\ldots,a_{x_3}}]$ is the Meijer's-G function [51], i.e.,

$$\mathcal{G}_{x_3,x_4}^{x_1,x_2}[y|_{b_1,\ldots,b_{x_4}}^{a_1,\ldots,a_{x_3}}] = \frac{1}{2\pi i}\cdot\int\frac{\prod_{j=1}^{x_1}\Gamma(b_j-x)\prod_{j=1}^{x_2}\Gamma(1-a_j+x)}{\prod_{j=x_1+1}^{x_4}\Gamma(1-b_j+x)\prod_{j=x_2+1}^{x_3}\Gamma(a_j-x)}y^x dx \tag{14}$$

4.2.1.2. VLC channel model. The VLC channel consists of both Line of Sight (LOS) component and Non Line of Sight (NLOS) component. LOS

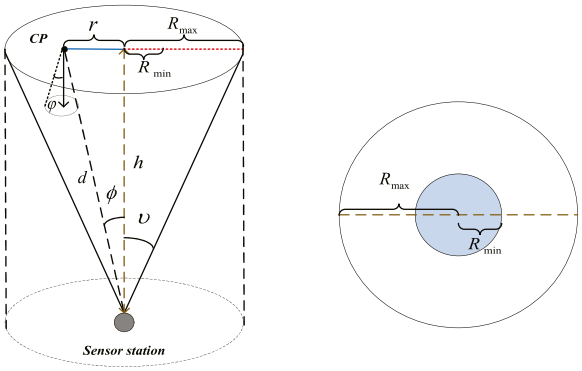

Fig. 3. The 3-D view of transmission between CP and sensor station using VLC channel and the location region of sensor station.

component provides a direct communication, while NLOS provides component the indirect communication of multiple reflections. Since the NLOS component only accounts for less than 4.94% of the total received signal at any particular instant [13,14], it can be assumed that the sensor station is only served by the best LOS link.

Based on the knowledge of VLC [9], the channel gain h_V of the LOS link between CP and a sensor station can be represented as

$$h_V = \frac{(\mathcal{M}+1)}{2\pi d^2} \cdot A \cdot R \cdot cos^{\mathcal{M}}(\varphi) \cdot cos(\varphi) \cdot U(\varphi) \cdot g(\varphi) \tag{15}$$

In Eq. (15), A and R denote the area and the responsivity of the detector at the sensor station [9], d represents the Euclidean distance between the sensor station and CP, φ and φ are the angle of irradiance and the angle of incidence, $U(\varphi)$ the optical filter's gain, and $g(\varphi)$ the gain of the optical concentrator (the angles are labeled in Fig. 3), $\mathcal{M}$ is the Lambertian pattern of the radiation [13,14], which is given by

$$\mathcal{M} = -\frac{1}{\log_2(cos(\upsilon))} \tag{16}$$

where υ is the semi-angle of LED used by sensor station (shown in Fig. 3).

Let h be the vertical distance between CP and the sensor stations' plane, r the projection distance of d (shown in Fig. 3), and $\mathcal{K} = \frac{ARU(\varphi)g(\varphi)}{2\pi}$, we can rewrite Eq. (15) as (noting $d^2 = h^2 + r^2$ and $cos(\varphi) = cos(\varphi) = \frac{h}{d}$)

$$h_V = \frac{(\mathcal{M}+1)h^{\mathcal{M}+1}\mathcal{K}}{(r^2+h^2)^{\frac{\mathcal{M}+3}{2}}} \tag{17}$$

If the position of sensor station follows a uniform distribution within the plane of a circular ring (see Fig. 3), the CDF of a sensor station's position $F_r(r)$ can be expressed as

$$F_r(r) = \frac{r^2 - R_{min}^2}{R_{max}^2 - R_{min}^2}, \quad R_{min} \le r \le R_{max} \tag{18}$$

where R_{max} denotes the radius of the circular plane determined by LED's coverage range, and R_{min} the minimum radius (R_{min} is generally set as zero [9,13,14]).

Using the conclusions of Eq. 17-Eq. (18), the PDF of VLC channel gain $g_V(h_V)$ can be accordingly derived as

$$g_V(h_V) = \frac{2\mathcal{K}^{\frac{2}{\mathcal{M}+3}} \cdot ((\mathcal{M}+1)h^{\mathcal{M}+1})^{\frac{2}{\mathcal{M}+3}} \cdot h_V^{-\frac{2}{\mathcal{M}+3}-1}}{(\mathcal{M}+3)(R_{max}^2 - R_{min}^2)} \tag{19}$$

Let γ_V be the SNR of VLC channel, E_v the transmission power of VLC channel, n_v the noise spectral density in the VLC channel, W_v the base band modulation bandwidth, and η the electrical-to-optical conversion efficiency, then γ_V is given as

$$\gamma_V = \eta^2 \cdot \frac{E_v^2 |h_V|^2}{n_v W_v} \tag{20}$$

As a consequence, the PDF $g_\gamma(.)$ of SNR of VLC channel is written as

$$g_\gamma(\gamma_V) = \frac{\mathcal{K}^{\frac{2}{\mathcal{M}+3}} \cdot [(\mathcal{M}+1)h^{\mathcal{M}+1}]^{\frac{2}{\mathcal{M}+3}} \cdot \left[\frac{n_v W_v \gamma_V}{E_v^2 \eta^2}\right]^{-\frac{1}{\mathcal{M}+3}}}{\gamma_V \cdot (\mathcal{M}+3) \cdot (R_{max}^2 - R_{min}^2)}$$
$$\gamma_V \in [\Xi_{min}, \Xi_{max}] \tag{21}$$

where Ξ_{min} and Ξ_{max} are respectively developed as

$$\Xi_{min} = \left[\frac{(\mathcal{K}(\mathcal{M}+1)h^{\mathcal{M}+1})^2}{(R_{max}^2 + h^2)^{\mathcal{M}+3}}\right] \cdot \eta^2 \cdot \frac{E_v^2}{n_v W_v} \tag{22}$$

$$\Xi_{max} = \left[\frac{(\mathcal{K}(\mathcal{M}+1)h^{\mathcal{M}+1})^2}{(R_{min}^2 + h^2)^{\mathcal{M}+3}}\right] \cdot \eta^2 \cdot \frac{E_v^2}{n_v W_v} \tag{23}$$

Integrating the function of Eq. (21), the CDF of SNR using VLC channel $G_\gamma(\gamma_V)$ can be represented as

$$G_\gamma(\gamma_V) = \frac{-\mathcal{K}^{\frac{2}{\mathcal{M}+3}}[(\mathcal{M}+1)h^{\mathcal{M}+1}]^{\frac{2}{\mathcal{M}+3}}}{(R_{max}^2 - R_{min}^2)} \cdot \left[\frac{n_v W_v \gamma_V}{E_v^2 \eta^2}\right]^{-\frac{1}{\mathcal{M}+3}} + \left[\frac{R_{max}^2 + h^2}{(R_{max}^2 - R_{min}^2)}\right] \tag{24}$$

Thus, we can rewrite Eq. (3) as

$$\begin{cases} P_{out}^{PLC} = Prb\{\gamma_P \le \zeta_p\} = F_\gamma(\zeta_p) \\ P_{out}^{V\,LC} = Prb\{\gamma_V \le \zeta_v\} = G_\gamma(\zeta_v) \end{cases} \tag{25}$$

4.2.2. MAC layer model

The MAC layer model is constructed based on the following assumptions:

(1) The transit buffer size of each sensor station is finite (denoted by K), and packets would be rejected because of overflow of the transit buffer (defined as overflow probability P_{OF});
(2) The HoL (head of line) packet transmission attempt process of one sensor station is independent of the other $N-1$ sensor stations [27,28], and the collision happens at PLC (or VLC) channel with a probability p_p (or p_v);
(3) The CP station has an infinite transmission buffer size, and it can receive transmitted packets from the sensor station regardless of whether a PLC channel or a VLC channel is used.

Now we establish the Double-Folding Heterogeneous Discrete Markov Chain (DFH DMC) model to depict the CSMA/CA process of HPVC MAC (please see Fig. 4). Since a sensor station can adopt PLC or VLC channel to transmit its HoL packet, the DFH DMC model consists of two parts: the CSMA/CA of IEEE 802.15.7 (the left area of Fig. 4) and the CSMA/CA of IEEE 1901 (the right area of Fig. 4). They are correlated by the channel selection probabilities P_{PLC} and P_{VLC} (derived in previous part). $B_{i,j}^t$ ($t \in [1, m]$, $i \in [1, d_t]$, $j \in [1, Q_t]$) and $b_{h,s}$($h \in [1, l]$, $s \in [1, W_h]$) in Fig. 4 denote the steady state probabilities [52] of the DFH DMC model (corresponding to the execution processes of IEEE 1901 and IEEE 802.15.7).

Let P_N be the steady state probability that the transit buffer of sensor station is not empty, the transmission attempt probability of a sensor station using PLC (or VLC) channel τ_p (or τ_v) can be expressed based on the DFH DMC model, i.e.,

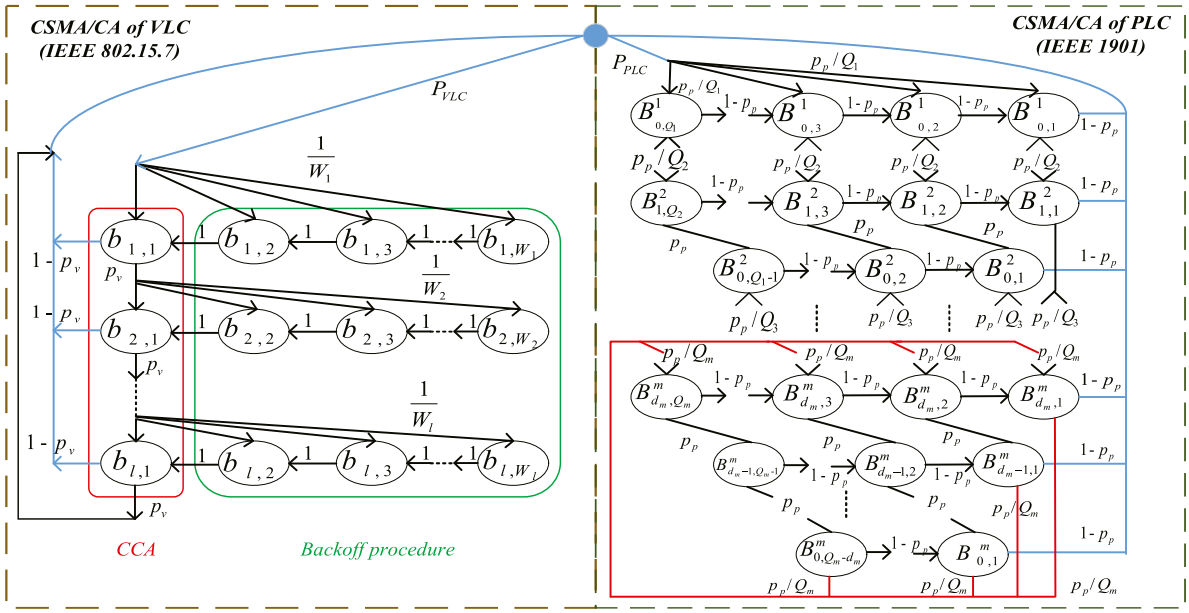

Fig. 4. The double-folding heterogeneous discrete Markov chain (DFH DMC) model for HPVC MAC protocol.

$$\begin{cases} \tau_p = \left[\dfrac{\sum_{t=1}^{m} \sum_{i=0}^{d_t} B_{i,1}^{t}}{\sum_{t=1}^{m} \sum_{i=0}^{d_t} \sum_{j=1}^{Q_t-(d_t-i)} B_{i,j}^{t}} \right] \cdot P_N \\ \tau_v = \left[\dfrac{\sum_{h=1}^{l} b_{h,1}}{\sum_{h=1}^{l} \sum_{s=1}^{W_l} b_{h,s}} \right] \cdot P_N \end{cases} \tag{26}$$

Applying the results given in our previous work [41], τ_p can be developed as

$$\tau_p = \left\{ \frac{\frac{1}{(1-p_p)}}{\sum_{i=1}^{m-1} Z_i \prod_{j=1}^{i-1} \chi_j + \prod_{j=1}^{m-1} \chi_{j\frac{Z_m}{(1-\chi_m)}}} \right\} \cdot P_N \tag{27}$$

where p_p is the conditional collision probability of competing for the PLC channel, Z_i represents the average number of time slots spent at backoff stage i (using IEEE 1901) and χ_i signifies the probability that a station enters into the next stage from backoff stage i (caused by unsuccessful attempt or DCP of 1901). Here Z_i and χ_i can be respectively represented as

$$\begin{cases} Z_i = \dfrac{1}{Q_i} \sum_{j=d_i+1}^{Q_i} [j(1-X_j^i)] + \\ \dfrac{1}{Q_i} \sum_{j=d_i+1}^{Q_i} \sum_{e=d_i+1}^{k} e[X_e^i - X_{e-1}^i] + \sum_{j=1}^{d_i} \dfrac{j}{Q_i}; \\ \chi_i = 1 - \left[\sum_{j=1}^{d_i} \dfrac{1}{Q_i} + \dfrac{1}{Q_i} \cdot \sum_{j=d_i+1}^{Q_i} (1-X_j^i) \right] + \\ p_p \cdot \left[\sum_{j=1}^{d_i} \dfrac{1}{Q_i} + \dfrac{1}{Q_i} \cdot \sum_{j=d_i+1}^{Q_i} (1-X_j^i) \right] \end{cases} \tag{28}$$

In Eq. (28), X_j^i denotes the probability of triggering DCP of 1901 and spending no more than j time slots at stage i, i.e.,

$$X_j^i = \sum_{t=d_i+1}^{j} \binom{j}{t} {p_p}^t (1-p_p)^{j-t} \tag{29}$$

Similarly, τ_v can be further written as

$$\tau_v = \frac{\left(\sum_{i=0}^{l-1} p_v^i\right)}{\sum_{i=1}^{l} p_v^{i-1}(1+W_i)/2} \cdot P_N \tag{30}$$

where p_v is the conditional collision probability of competing for the VLC channel.

The probability p_{tr}^{Φ} that at least one sensor station tries to a transmission through Φ channel (Φ is the indicative symbol, $\Phi = p$ means PLC channel, while $\Phi = v$ represents VLC channel), and the probability p_{idle}^{Φ} that Φ channel is idle can be expressed respectively as

$$p_{tr}^{\Phi} = 1 - (1-\tau_{\Phi})^{N_{\Phi}}, \quad \Phi \in \{p, v\} \tag{31}$$

$$p_{\text{idle}}^{\Phi} = 1 - p_{tr}^{\Phi} = (1-\tau_{\Phi})^{N_{\Phi}}, \quad \Phi \in \{p, v\} \tag{32}$$

where N_{Φ} denotes the number of sensor stations competing for the Φ channel, i.e.,

$$\begin{cases} N_p = N \cdot P_{PLC}, & \Phi = p \\ N_v = N \cdot P_{V\,LC}, & \Phi = v \end{cases} \tag{33}$$

Then, the relationship between the transmission attempt probability τ_{Φ} and the conditional collision probability p_{Φ} using Φ channel can be expressed as the following fixed point equation

$$p_{\Phi} = 1 - (1-\tau_{\Phi})^{N_{\Phi}-1}, \quad \Phi \in \{p, v\} \tag{34}$$

Remark 2. Reviewing the above analysis, the detailed expansion form of P_N is still unknown, and it relies on the mixed packet queueing process in the transit buffer (since a sensor station can choose PLC or VLC channel to finish the data transmission). Thus, we further employ Queueing dynamics to express P_N, and derive the system metrics of HPVC MAC.

4.2.3. System metrics of HPVC MAC

Because of the introduction of CS strategies, a sensor station has a mixture medium service mode, therefore we cannot directly use the Queueing modeling part of our previous works [41,42]. Let $E[U]$ be the average service rate of a sensor station, we have

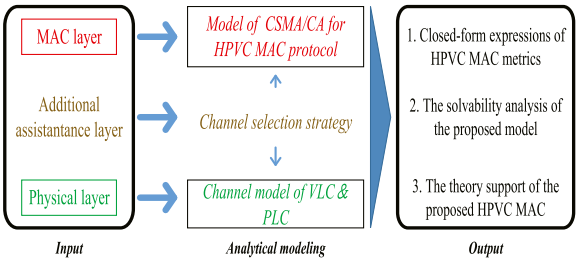

Fig. 5. The overall modeling process.

$$\frac{1}{E[U]} = P_{PLC} \cdot \frac{1}{E[U_p]} + P_{V\,LC} \cdot \frac{1}{E[U_v]} \tag{35}$$

where $E[U_p]$ denotes the average service rate of a sensor station using PLC channel, and $E[U_v]$ the average service rate of a sensor station using VLC channel, respectively. Furthermore, $\frac{1}{E[U]}$ is equivalent to the average MAC service time of HPVC networks.

To get the expansion expression of $E[U]$, we firstly derive $E[U_v]$. Based on the proposed DFH DMC model, the service time distribution probability under VLC channel $Prb\{\frac{1}{U_v} = T_v(t)\}$ can be given by

$$Prb\left\{\frac{1}{U_v} = T_v(t)\right\} = \begin{cases} p_v^{t-1} \cdot (1-p_v), t \in [1, l] \\ p_v^l \end{cases} \tag{36}$$

In Eq. (36), the first sub-formula means that the successful transmission occurs at backoff stage t, while the second sub-formula denotes that the packet is finally dropped after the lth transmission attempt failure. In addition, the corresponding average spent time $\frac{1}{U_v} = T_v(t)$ can be further computed as [28].

$$\frac{1}{U_v} = T_v(t) = \begin{cases} T_S + (t-1)T_C + tT_{CS} + \sum_{i=1}^{t} UBP \cdot \frac{W_i - 1}{2}, t \in [1, l] \\ l \cdot T_C + l \cdot T_{CS} + \sum_{i=1}^{l} UBP \cdot \frac{W_i - 1}{2} \end{cases} \tag{37}$$

where UBP denotes one unit bakcoff period (20 optical clocks [28]), T_{CS} the channel sensing time (i.e., the duration of CCA, 8 optical clocks [28]), T_S the successful transmission time duration, T_C the collision time duration, respectively.

According to the time frame setting of IEEE 802.15.7 protocol [28], T_S and T_C are given by

$$\begin{cases} T_S = t_d + t_{ACK} + t_{IFS} + 2t_{prop} + \Delta \\ T_C = t_d + t_{ACK-to} + t_{prop} \end{cases} \tag{38}$$

where t_d represents the data frame duration, t_{IFS} the inter-frame space, t_{ACK} the Acknowledge frame duration, t_{ACK-to} the ACK waiting time and t_{prop} the propagation delay, respectively (Δ is the channel selection time defined previously).

Remark 3. The sensor station can always receive an ACK frame after the packet is successfully accepted or received in outage by the CP station (regardless of using PLC channel or VLC channel).

Then $E[U_v]$ is accordingly expressed as

$$E[U_v] = \left[\sum Prb\left\{\frac{1}{U_v} = T_v(t)\right\} \cdot \left[\frac{1}{U_v} = T_v(t)\right]\right]^{-1} \tag{39}$$

Similarly, we can obtain the expression of $E[U_p]$ (the derivation process is shown in **Appendix A**). It is noted that the time frames of IEEE 1901 protocol are given in **Appendix A** (the readers can also refer to Refs. [27,35–42]).

Through the above analysis, we can finally obtain the expression of $E[U]$. Further use of $M/M/1/K$ queueing model [52], P_N is approximately expressed as

$$P_N \doteq 1 - \frac{\left(1 - \frac{\lambda}{E[U]}\right)}{1 - \left(\frac{\lambda}{E[U]}\right)^{K+1}} \tag{40}$$

Moreover, the steady state probability $\mathcal{Q}_x$ that there are x packets in the transit buffer can be written as

$$\mathcal{Q}_x \doteq \frac{\left(1 - \frac{\lambda}{E[U]}\right)\left(\frac{\lambda}{E[U]}\right)^x}{1 - \left(\frac{\lambda}{E[U]}\right)^{K+1}}, x \in [0, K] \tag{41}$$

Remark 4. Because of the working principle of HPVC MAC, it's hard to derive the accurate expressions of P_N and $\mathcal{Q}_x$. Hence, we adopt the $M/M/1/K$ model (an approximate method) [52] to simplify the derivation.

The average queue length $E[\mathcal{Q}]$ and the overflow probability of the transit buffer P_{OF} can be accordingly derived as

$$E[\mathcal{Q}] = \sum_{x=0}^{K} \mathcal{Q}_x \cdot x \tag{42}$$

$$P_{OF} = \mathcal{Q}_K = \frac{\left(1 - \frac{\lambda}{E[U]}\right)\left(\frac{\lambda}{E[U]}\right)^K}{1 - \left(\frac{\lambda}{E[U]}\right)^{K+1}} \tag{43}$$

Considering the retransmission limit of executing IEEE 802.15.7 protocol in VLC component [28], the packet drop probability p_{dp} at MAC layer is given as

$$p_{dp} = \frac{p_v^l}{\sum_{i=1}^{l} p_v^{i-1}(1 + W_i)/2} \cdot P_N \cdot N_v \tag{44}$$

Moreover, the successful transmission probability P_s^{Φ} using $\Phi \in \{p, v\}$ channel, and total successful transmission probability PS can be expressed as

Table 2
VLC component parameters.

VLC Channel layer	Size [13,14]
υ (semi-angle of LED)	$\pi/3$
$U(\varphi)$ (optical filter's gain)	1
$g(\varphi)$ (gain of the optical concentrator)	1
A (area of the detector)	$10^{-4}\ m^2$
R (responsivity of the detector)	1
h (height)	$5\ m$
$R_{\min}$ (minimum radius)	$0\ m$
$R_{\max} = h \cdot \tan\upsilon$ (maximum radius)	$5\sqrt{3}\ m$
r (projection distance of sensor station)	$5\sqrt{2}\ m$
η (electrical-to-optical conversion efficiency)	0.80 A/W
W_v (base band modulation bandwidth)	2×10^6 Hz
E_v (transmission power of VLC)	1 w
n_v (noise spectral density of VLC)	$10^{-21}\ A^2$/Hz
VLC MAC layer (IEEE 802.15.7)	**Size [44,47]**
duration of one optical clock	$1/(2 \times 10^5)$ s
UPB (unit backoff period)	20 optical clocks
T_{CS} (channel sensing time)	8 optical clocks
t_{ACK} (acknowledgment frame duration)	12 optical clocks
t_{ACK-to} (acknowledgment waiting time)	120 optical clocks
t_{IFS} (inter-frame space)	40 optical clocks
t_{prop} (propagation delay)	$1/(3 \times 10^8)$ s
Δ (channel selection duration)	$5\ \mu s$
l (maximum backoff stage)	5
BE (backoff exponent)	[4,7]

Table 3
PLC component parameters.

PLC Channel layer	Size [9,13]
ρ (arrival rate of occurrence of impulsive noise)	10
T (duration of occurrence of impulsive noise)	0.01 s
β (noise ratio)	5
σ_B^2 (average background noise power)	0.1 w
E_p (transmission power of PLC)	1 w
m_1, m_2 (export parameters, Eq. (12))	1.55
μ_p (scale parameter of PLC channel)	0.1
PLC MAC layer (IEEE 1901)	**Size [39,41]**
Slot(σ)	35.84 μs
PRS (Priority slot)	35.84 μs
PR (Preamble)	110.48 μs
CIFS (contention inter-frame space)	100.00 μs
RIFS (response inter-frame space)	140.00 μs
ACK (acknowledgment frame duration)	110.48 μs
EIFS (extended inter-frame space)	2920.64 μs
R_p (medium bit rate of PLC)	2 Mbps

$$\begin{cases} P_s^p = N_p \cdot \tau_p (1-\tau_p)^{N_p-1} \cdot (1 - F_\gamma(\zeta_p)) \\ P_s^v = N_v \cdot \tau_v (1-\tau_v)^{N_v-1} \cdot (1 - G_\gamma(\zeta_v)) \\ PS = P_s^p + P_s^v \end{cases} \tag{45}$$

Thus, we can write the Goodput [42] of HPVC networks Gp as

$$Gp = \frac{PS \cdot L}{\frac{1}{E[U]}} = PS \cdot L \cdot E[U] \tag{46}$$

Let Q_s be the Quality of Information (QoI) value of a data packet (generally, the large value of QoI indicates a high transmission reward) [32,33], the expected QoI of one successful transmission $E[Q_s]$ for HPVC networks can be given by

$$\begin{aligned} E[Q_s] &= Q_s \cdot PS \\ &= Q_s \cdot \left[N_p \tau_p (1-\tau_p)^{N_p-1} (1 - F_\gamma(\zeta_p)) + N_v \tau_v (1-\tau_v)^{N_v-1} (1 - G_\gamma(\zeta_v)) \right] \end{aligned} \tag{47}$$

It's easy to find that $E[Q_s]$ has the upper bound performance (see **Appendix B**).

4.3. Solvability analysis of the proposed joint analytical model

In this section, we will analyze whether the joint analysis model is solvable. Given the impact of the CS strategy, this problem can be divided into two parts, i.e., solvability judgment after selecting the PLC channel and solvability judgment after selecting the VLC channel.

Remark 5. The solvability judgement after choosing PLC channel is similar to the content given in our previous work [49], thus we do not make the verification any more.

Rewrite Eq. (34) as $p_v = \Theta(\tau_v(p_v))$, then a relaxed iteration equation [53] can be constructed for p_v, i.e.,

$$p_v(\alpha+1) = (1-\Lambda)\Theta(\tau_v(p_v(\alpha))) + \Lambda p_v(\alpha), \Lambda \in (0,1) \tag{48}$$

where α represents the iteration times.

According to Weak Convergence theory [53], if $[\Theta(\tau_v(p_v))]'$ is bounded and $\Theta(\tau_u(p_v(\alpha))) \le p_v(\alpha)$, $p_v(\alpha)$ can converge to a general fixed point p_v, i.e., the model after choosing VLC channel has the solvability.

Taking the derivative for Eq. (30), we have

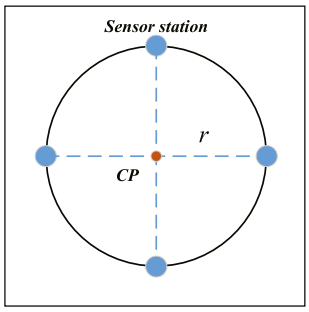

Fig. 6. A simple case of HPVC network including four sensor stations and a CP station (top view).

$$\begin{aligned} \tau_v'(p_v) = &\left[\frac{\left(\sum_{i=0}^{l-1} p_v^i\right)}{\sum_{i=1}^{l} p_v^{i-1}(1+W_i)/2} \right]' \cdot P_N + \\ &\left[\frac{\left(\sum_{i=0}^{l-1} p_v^i\right)}{\sum_{i=1}^{l} p_v^{i-1}(1+W_i)/2} \right] \cdot P_N' \end{aligned} \tag{49}$$

Based on the expansion form of Eq. (49), the following inequations can be straightforwardly obtained

$$\begin{cases} P_N = 1 - \dfrac{1-(\lambda/E[U])}{1-(\lambda/E[U])^{K+1}} < 1 \\ \dfrac{\left(\sum_{i=0}^{l-1} p_v^i\right)}{\sum_{i=1}^{l} p_v^{i-1}(1+W_i)/2} < \dfrac{1}{(1+W_1)/2} \\ \left[\dfrac{\left(\sum_{i=0}^{l-1} p_v^i\right)}{\sum_{i=1}^{l} p_v^{i-1}(1+W_i)/2} \right]' \le 0 \end{cases} \tag{50}$$

Further deriving the expression of P_N', we have

$$\begin{aligned} P_N' &= \left(1 - \frac{1-(\lambda/E[U])}{1-(\lambda/E[U])^{K+1}}\right)' = -\left[\frac{1}{\sum_{x=0}^{K}\left(\frac{\lambda}{E[U]}\right)^x}\right]' \\ &= \frac{\sum_{x=1}^{K}\left(x \cdot \frac{\lambda}{E[U]}\right)^{x-1}}{\left[\sum_{x=0}^{K}\left(\frac{\lambda}{E[U]}\right)^x\right]^2} \cdot \lambda \cdot \left[\frac{1}{E[U]}\right]' \le \lambda \cdot \left[\frac{1}{E[U]}\right]' \end{aligned} \tag{51}$$

It's easy to conclude that if $\left[\frac{1}{E[U]}\right]'$ is bounded, P_N' would be bounded as well. Reviewing the derivation process of $\frac{1}{E[U_v]}$, the first order derivative of $\frac{1}{E[U_v]}$ can be expressed as

$$\left[\frac{1}{E[U_v]}\right]' = \sum \left[Prb\left\{\frac{1}{U_v} = T_v(t)\right\}\right]' \cdot T_v(t) \tag{52}$$

where $[Prb\{\frac{1}{U_v} = T_v(t)\}]'$ is written as

$$\left[Prb\left\{\frac{1}{U_v} = T_v(t)\right\}\right]' = \begin{cases} (t-1)\cdot p_v^{t-2} - t \cdot p_v^{t-1}, t \in [1, l] \\ l \cdot p_v^{l-1} \end{cases} \tag{53}$$

Clearly, $[Prb\{\frac{1}{U_v} = T_v(t)\}]'$ always has the upper bound value, i.e.,

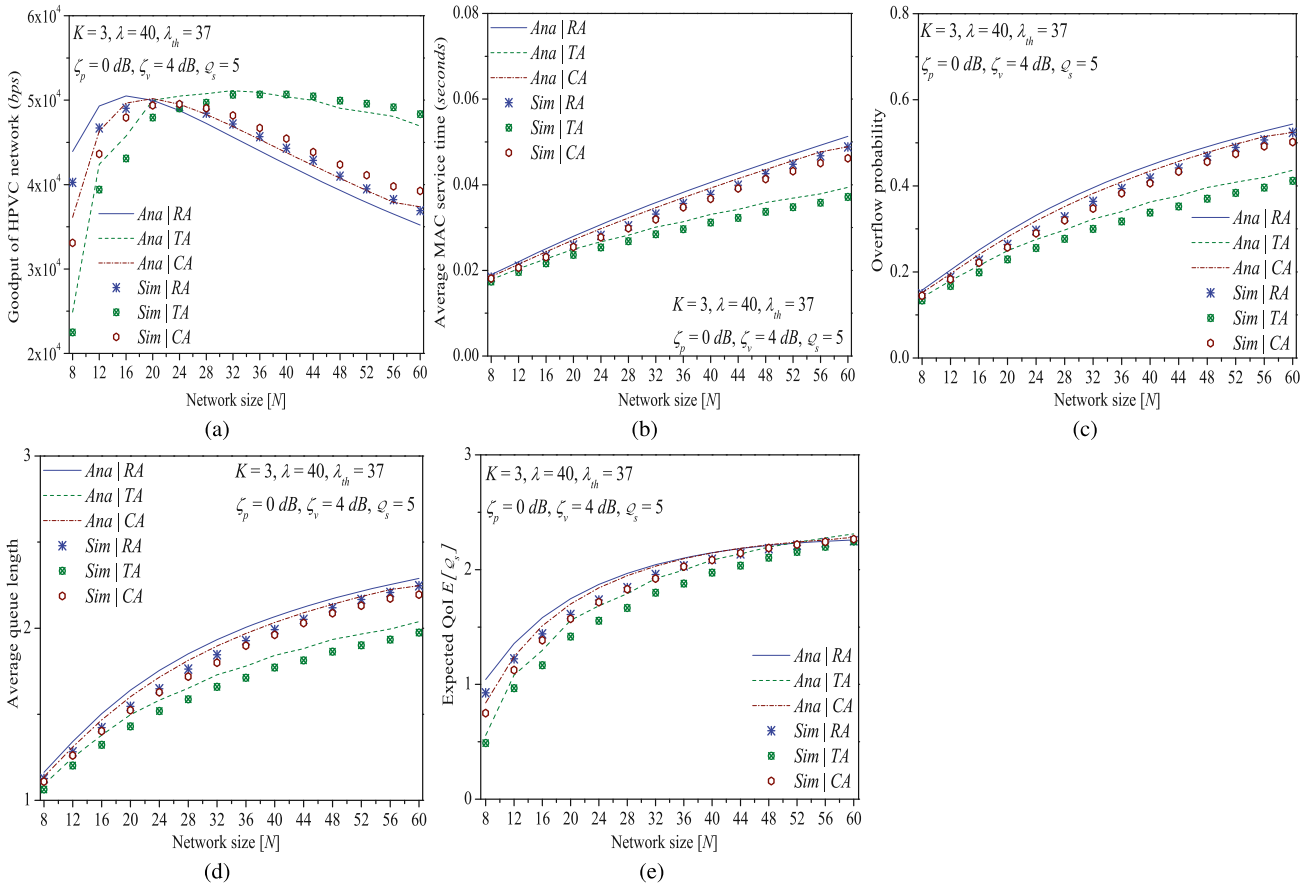

Fig. 7. HPVC MAC's performance under different network sizes.

$$\begin{cases} \left[Prb\left\{\dfrac{1}{U_v}=T_v(t)\right\}\right]' \le 0 \quad |t=1 \\ \left[Prb\left\{\dfrac{1}{U_v}=T_v(t)\right\}\right]' \le \left[Prb\left\{\dfrac{1}{U_v}=T_v(t)\right\}\middle| p_v=\dfrac{t-2}{t}\right]' \\ |t\in[2,l]; \\ \left[Prb\left\{\dfrac{1}{U_v}=T_v(t)\right\}\right]' \le l \end{cases} \tag{54}$$

As a consequence, we can determine that $\left[\frac{1}{E[U_v]}\right]'$ is bounded, i.e., $\left[\frac{1}{E[U_v]}\right]' \le A_1$ (A_1 is a positive constant).

Similarly, we can reach the conclusion that $\left[\frac{1}{E[U_p]}\right]'$ is bounded (using the method given in Eq. 49-Eq. (54)), i.e., $\left[\frac{1}{E[U_p]}\right]' \le A_2$ (A_2 is a positive constant).

Thus, we derive the following inequations (noting A_3 in Eq. (56) is a positive constant):

$$\left[\frac{1}{E[U]}\right]' = P_{V\,LC}\cdot\left[\frac{1}{E[U_v]}\right]' + P_{PLC}\cdot\left[\frac{1}{E[U_p]}\right]' \le P_{V\,LC}\cdot A_1 + P_{PLC}\cdot A_2 \tag{55}$$

$$\begin{aligned} [\Theta(\tau_v(p_v))]' &= (N_v-1)(1-\tau_v(p_v))^{N_v-2}\cdot[\tau_v(p_v)]' \\ &\le (N_v-1)\cdot\frac{1}{(1+W_1)/2}\cdot P_N' \\ &\le (N_v-1)\cdot\frac{1}{(1+W_1)/2}\cdot\lambda\cdot\left[\frac{1}{E[U]}\right]' \\ &\le (N_v-1)\cdot\frac{\lambda}{(1+W_1)/2}\cdot(P_{V\,LC}\cdot A_1 + P_{PLC}\cdot A_2) = A_3 \end{aligned} \tag{56}$$

In other words, $[\Theta(\tau_v(p_v))]'$ is bounded.

Next, we utilize recursion method to prove $\Theta(\tau_v(p_v(\alpha))) \le p_v(\alpha)$. Assuming $\Theta(\tau_v(p_\alpha)) \le p_\alpha$ holds, $\Theta(\tau_v(p_{\alpha+1})) - p_{\alpha+1}$ can be computed as

$$\begin{aligned} &\Theta(\tau_v(p_v(\alpha+1))) - p_v(\alpha+1) \overset{a}{=} \Theta(\tau_v(p_v(\alpha+1))) - [(1-\Lambda)\Theta(\tau_v(p_v(\alpha))) + \Lambda p_v(\alpha)] \\ &\overset{b}{=} [\Theta(\tau_v(p_v(\alpha+1))) - \Theta(\tau_v(p_v(\alpha)))] + \Lambda\cdot[\Theta(\tau_v(p_v(\alpha))) - p_v(\alpha)] \\ &\overset{c}{=} \Theta'(\tau_v(\varrho))(p_v(\alpha+1) - p_v(\alpha)) + \Lambda[\Theta(\tau_v(p_v(\alpha))) - p_v(\alpha)] \\ &\overset{d}{\le} A_3[p_v(\alpha+1) - p_v(\alpha)] + \Lambda[\Theta(\tau_v(p_v(\alpha))) - p_v(\alpha)] \\ &\overset{e}{=} A_3(1-\Lambda)[\Theta(\tau_v(p_v(\alpha))) - p_v(\alpha)] + \Lambda\cdot[\Theta(\tau_v(p_v(\alpha))) - p_v(\alpha)] \\ &\overset{f}{=} [\Lambda + A_3(1-\Lambda)][\Theta(\tau_v(p_v(\alpha))) - p_v(\alpha)] \le 0 \end{aligned} \tag{57}$$

where the "c"th line is derived using the conclusions of Lagrange's mean value theorem and Eq. (56) (ϱ is between $p_v(\alpha)$ and $p_v(\alpha+1)$).

Since $\Theta(\tau_v(p_v))$ is continuous with respect to p_v [53], the bounded and non-increasing sequence must converge to a general fixed point of p_v. In other words, the proposed analytical model after choosing VLC channel is solvable.

Likewise, the analytical model after choosing PLC channel is also solvable (proved by using the conclusion of our previous work [49]). Thus, we can totally assert that the joint analytical model of HPVC MAC has the solvability.

Now we use Fig. 5 to summarize the overall modeling process.

5. Performance evaluation

To evaluate the performance of HPVC MAC protocol, and verify the correctness of the corresponding analytical model, we construct simula-

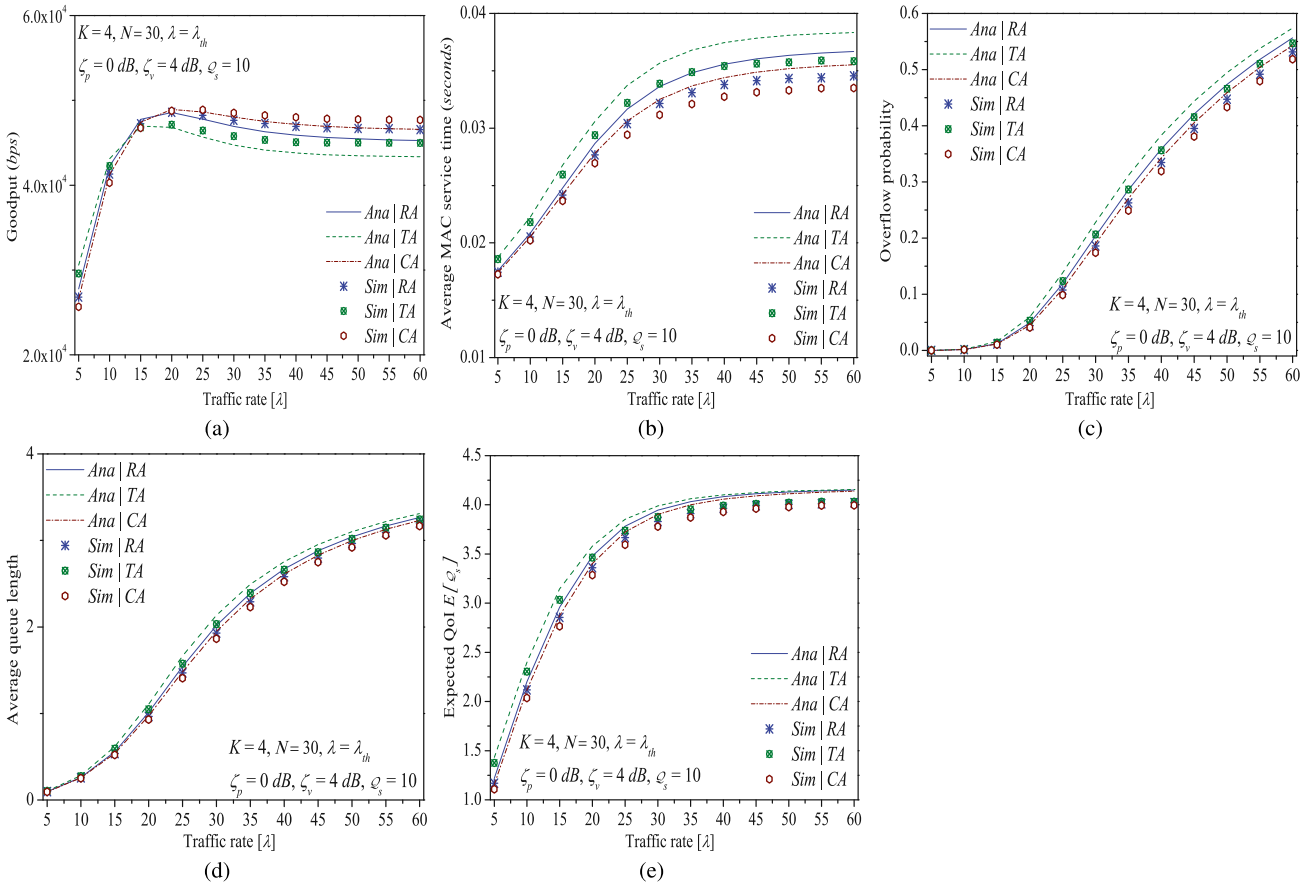

Fig. 8. HPVC MAC's performance under different traffic rates.

tion scenarios using Matlab (R2015a) on a PC with intel i7-6500 cpu, 2.50 GHz, 8 GB RAM. The HPVC MAC protocol is implemented by introducing the CS strategies and incorporating the standards of IEEE 802.15.7 and IEEE1901.[3] The parameters used in simulation are shown in Tables 1–3. In the simulation, the HPVC network is represented as a star-shaped topology with N sensor stations (having the same projection distance r) and a CP station for receiving data packets (see the simple case of Fig. 6). Each sensor station generates packets based on Poisson process at an average rate λ. Sensor stations transmit their data packets to the CP station through PLC and VLC channels. The channel fading types of PLC and VLC channels are described in Section 4.2, and the arrival of additive impulsive noise in PLC channel follows a discrete Poisson process scaled by T and ρ. All sensor stations adopt the same priority type ($CA0/CA1$) [27] and transit buffer size K, and the packet size is fixed as $L = 500$ Bytes.[4] Each simulation experiment unit runs 10^6 time slots (the duration of one time slot in simulation is set as 3×10^3 μs). All simulation results are with 0.95 confidence interval between$[0.93Avg(.), 1.07Avg(.)]$, where $Avg(.)$ represents the average simulation result. With the help of relax iteration algorithm [54] (it's also available to use **fsolve** function of Matlab), the joint analytical model is solved (i.e., computing the collision probability $p_\Phi|\Phi \in \{p, v\}$). The cut-off precision [54] of calculating one group $p_\Phi|\Phi \in \{p, v\}$ is set as 10^{-6}, and it requires approximately less than 80 s. The average error rate[5] between simulation and numerical analysis results is 4.62%. Furthermore, the Meijer's-G function (Eq. (13)) in the joint analytical model is solved by utilizing MuPad [55].

All experiments are divided into four groups: (1) the impact of network size N, (2) the impact of traffic rate λ, (3) the impact of transit buffer size K and (4) the impact of required minimum SNR ζ_p&ζ_v. In each group, we plot the MAC performance under three different CS strategies, including RA, TA and CA.[6]

In addition, the proposed HPVC MAC is measured through five different significant metrics:

(1) Goodput Gp: indicates the end to end data transmission rate of using HPVC MAC, reflecting the impact of MAC protocol on transmission efficiency;
(2) Average MAC service time $\frac{1}{E[U]}$: denotes the interval from when the packet becomes a HoL packet to when it is forwarded to the destination station, reflecting the service efficiency of using HPVC MAC protocol;
(3) Overflow probability P_{OF}: denotes the possibility that the transit buffer size is fully-loaded caused by executing HPVC MAC protocol;
(4) Average queue length $E[\mathcal{Q}]$: reflects the number of packets staying in the transit buffer waiting to execute HPVC MAC protocol;
(5) Expected QoI $E[Q_s]$: reflects the impacts of successful transmission probability of executing HPVC MAC and the information value of packet [32,33] on final transmission reward.

[3] The CSMA/CA mechanism of IEEE 1901 is achieved by modifying the backoff counter window of 802.11, and adding a parallel deferral counter window (executing the deferral counter process); while the CSMA/CA mechanism of IEEE 802.15.7 is realized by modifying the backoff process of 802.11.

[4] t_d and D can be straightforwardly derived by the value of L.

[5] The error rate is denoted as $|\frac{Sim-Ana}{Sim}|$, where Sim and Ana represent the simulation result and numerical analysis result, respectively.

[6] It should be stressed that we do not consider how to further optimize the MAC performance of HPVC networks in this paper.

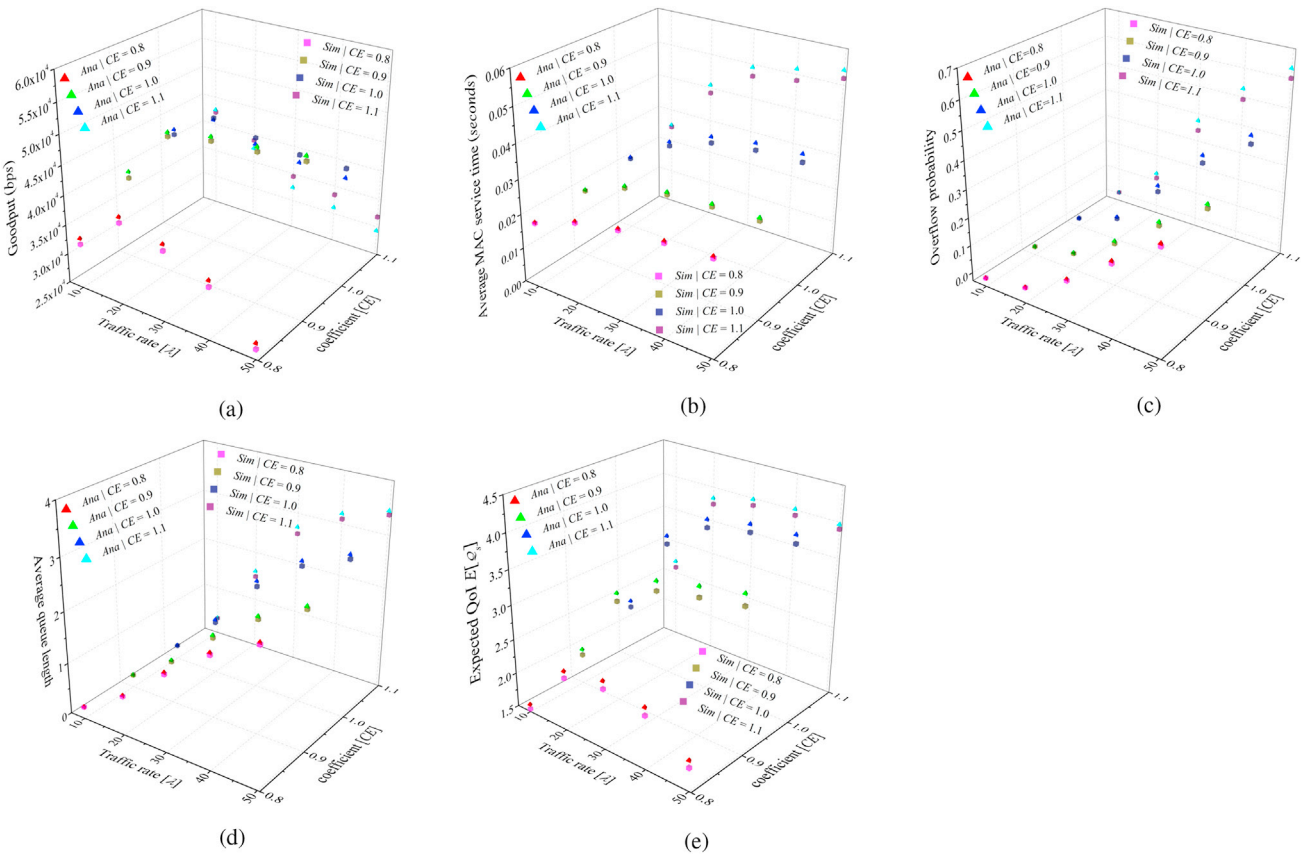

Fig. 9. The impact of λ_{th} on HPVC MAC with TA CS (3-dimension perspective).

5.1. The impact of network size

In this simulation group, we set the required minimum SNR $\zeta_p = 0$ dB&$\zeta_v = 4$ dB,[7] average traffic rate $\lambda = 40$, threshold traffic rate $\lambda_{th} = 37$, QoI $Q_s = 5$, transit buffer size $K = 3$, and the number of sensor stations N varies in [8, 60]. Fig. 7 shows the simulation and analysis results including the Goodput Gp, average MAC service time $\frac{1}{E[U]}$, overflow probability P_{OF}, average queue length $E[\mathcal{Q}]$ and expected QoI $E[Q_s]$ of HPVC MAC with different N.

With the increase of network size N, more sensor stations compete for PLC and VLC channels, thus the medium utilization is enhanced. However, as the medium contention continuously intensifies, the channel utilization would be degraded. As a result, we see the Goodput increases first, then decreases (it is affected not only by the total successful transmission probability PS but also by the average MAC service time $\frac{1}{E[U]}$). Since more sensor stations contend for the same medium (verified by Eq. (33)), the data packet needs to wait a longer time duration to get the medium service, and the transit buffer is easier to be fully loaded. Consequently, we find that the average MAC service time, overflow probability and average queue length increase with the increasing network size N. The expected QoI $E[Q_s]$ increases with the increasing network size N, because the network size is positively associated with $E[Q_s]$ (demonstrated by Eq. (47)).

It's clear that the introduced CS strategies would affect the performance of HPVC MAC protocol in this simulation group. Because different CS strategies would result in different values of P_{PLC} and P_{VLC} (reviewing Section 4), which ultimately determine the number of sensor stations contending PLC and VLC channels. Due to the utilization of $M/M/1/K$ model (an approximate method) in the derivation process, there exists an acceptable gap between simulation and numerical analysis results. Overall, the proposed conjoint analysis model is still sufficiently accurate.

Here is an example of Goodput Gp for HPVC MAC ($N \in [8, 60]$). The simulation results of Gp vary from 40.25 kbps to 49.61 kbps, then to 36.90 kbps using RA CS; from 22.49 kbps to 50.69 kbps, then to 48.34 kbps using TA CS; from 33.08 kbps to 49.54 kbps, then to 39.25 kbps using CA CS.

The numerical analysis results of Gp vary from 43.93 kbps to 50.52 kbps, then to 35.21 kbps using RA CS; from 24.88 kbps to 51.14 kbps, then to 46.92 kbps using TA CS; from 36.13 kbps to 50.18 kbps, then to 37.36 kbps using CA CS.

5.2. The impact of traffic rate λ

In this simulation group, we set the number of sensor stations $N = 30$, required minimum SNR $\zeta_p = 0$ dB&$\zeta_v = 4$ dB, QoI $Q_s = 10$, transit buffer size $K = 4$, and the average traffic rate λ varies in [5, 60] (threshold traffic rate $\lambda_{th} = \lambda$). Fig. 8 shows the simulation and numerical analysis results including the Goodput Gp, average MAC service time $\frac{1}{E[U]}$, overflow probability P_{OF}, average queue length $E[\mathcal{Q}]$ and expected QoI $E[Q_s]$ of HPVC MAC with different λ.

As the traffic rate λ increases, the transmission attempt frequency of sensor station increases (no matter using PLC or VLC channel), thus enhancing the channel utilization. However, with the transmission attempt frequency continuously intensifying, the collision frequency (including PLC and VLC components) increases correspondingly, and the

[7] Limited by the VLC parameter setting, γ_V can only vary in [3.067 dB, 27.150 dB].

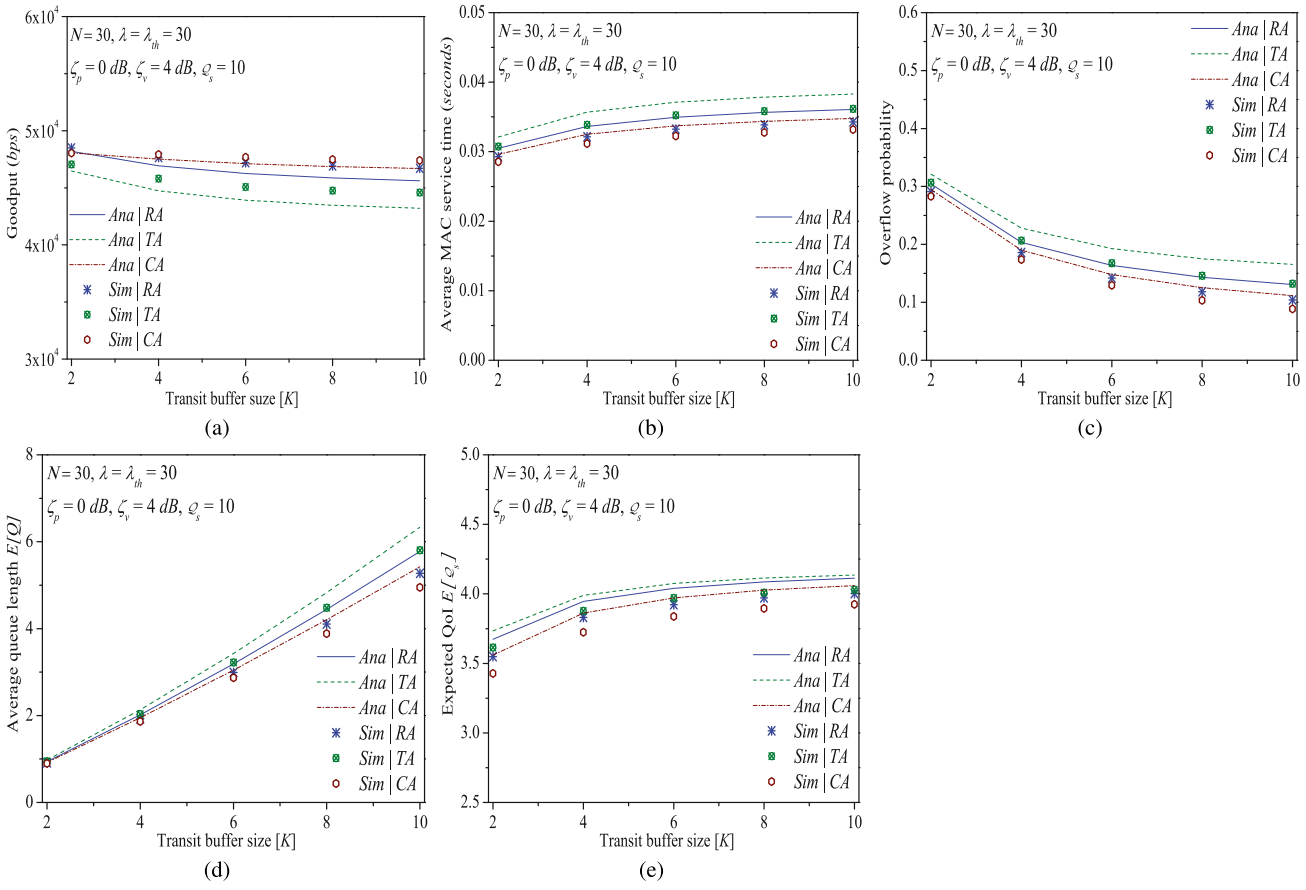

Fig. 10. HPVC MAC's performance under different transit buffer size.

channel utilization would be reduced until the "saturated state" is reached [39], i.e., the conditional collision probability $p_{\Phi}|\Phi \in \{p, v\}$ only slightly increases. Therefore, we see the Goodput increases first, then slowly decreases. The average MAC service time, overflow probability and average queue length increase with the traffic. That is because as λ increases, the competition frequency of PLC and VLC mediums increases, and accordingly the collision probabilities p_p and p_v increase. As a result, the data packet must wait longer to get the medium service, more packets would stay in the transit buffer, and the sensor station is also easier to be fully loaded. The expected QoI $E[Q_s]$ increases with the increasing λ. The most possible reason is that the total successful transmission probability PS, i.e., "$[N_p\tau_p(1-\tau_p)^{N_p-1}(1-F_\gamma(\zeta_p)) + N_v\tau_v(1-\tau_v)^{N_v-1}(1-G_\gamma(\zeta_v))]$" in Eq. (47) is monotonously increasing for $\lambda \in [5, 60]$ that accordingly leads to the change rule of $E[Q_s]$.

Similarly, the performance of HPVC MAC protocol in this simulation group is affected by the CS strategies (analyzed in Section 5.1). In addition, as the traffic rate increases (reaching "saturation"), the approximations used in the modeling process ($M/M/1/K$ model) will further reduce the accuracy of our proposed analytical model (for reasons that have been explained in Queueing theory [52, Chapter 7] and will not be repeated). Overall, a good fit between the simulation and numerical analysis results still exists.

Here is an example of average MAC service time $\frac{1}{E[U]}$ for HPVC MAC ($\lambda \in [5, 60]$). The numerical analysis results of $\frac{1}{E[U]}$ vary from 0.01757 s to 0.03668 s using RA CS; from 0.01875 s to 0.03833 s using TA CS; from 0.01739 s to 0.03553 s using CA CS.

The simulation results of $\frac{1}{E[U]}$ vary from 0.01745 s to 0.03457 s using RA CS; from 0.01860 s to 0.03584 s using TA CS; from 0.01726 s to 0.03350 s using CA CS.

Remark 6. It should be emphasized that the threshold traffic rate λ_{th} would also affect the performance of HPVC MAC using TA CS. Let CE denote the coefficient of λ_{th}, i.e., $\lambda = CE \cdot \lambda_{th}$. Fig. 9 plots the performance of HPVC MAC using TA CS under different ($\lambda \in [10, 50]$, $CE \in [0.8, 1.1]$) from the three-dimension perspective (the other parameter settings are unchanged). We can clearly find that the HPVC MAC performs differently under different values of CE. The reason is that λ_{th} affects the values of P_{PLC} and P_{VLC} (verified by Eq. (2)), which ultimately influence the performance of HPVC MAC.

5.3. The impact of transit buffer size K

In this simulation group, we set the number of stations $N = 30$, required minimum SNR $\zeta_p = 0$ dB&$\zeta_v = 4$ dB, average traffic rate $\lambda = 30$ (threshold traffic rate $\lambda_{th} = \lambda$, i.e., $CE = 1$), QoI $Q_s = 10$ and the transit buffer size K varies in Refs. [2,10]. Fig. 10 shows the simulation and numerical analysis results including the Goodput Gp, average MAC service time $\frac{1}{E[U]}$, overflow probability P_{OF}, average queue length $E[\mathcal{Q}]$ and expected QoI $E[Q_s]$ of HPVC MAC with different K.

As shown in Fig. 10, the performance of Goodput, average MAC service time, overflow probability, average queue length and expected QoI is affected by the size of transit buffer K. We can find that larger size of transit buffer would not result in superior performance of Goodput and MAC service time. The most possible reason is that with the increase of buffer size K, more packets enter into the transit buffer, and thereby have the chance of participating the medium contention instead of being directly blocked. As a result, the medium contention intensifies, and the average waiting time of packets for receiving the medium service increases, thus reducing the transmission efficiency, i.e., decreasing the Goodput Gp (verified by Eq. (46)). In addition, with the increasing K, the transit buffer is no longer prone to be full, and it has the capability of holding more packets. Therefore, the overflow probability decreases, and

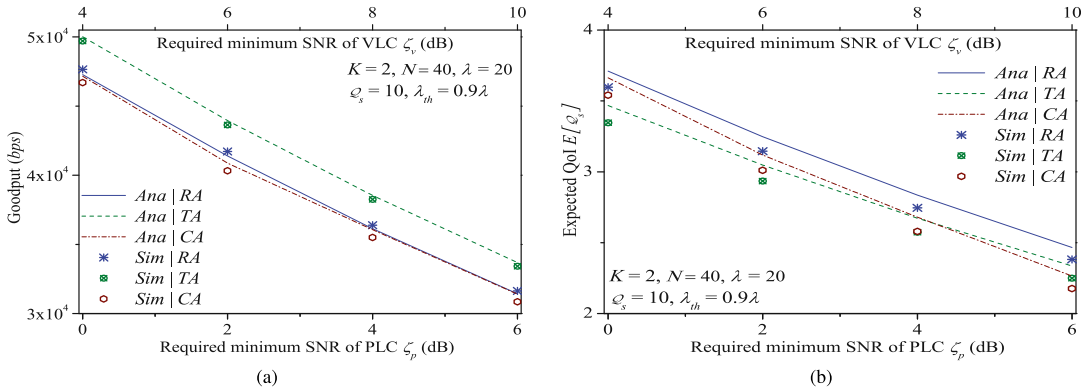

Fig. 11. The impacts of required minimum SNR on Goodput and Expected QoI for HPVC MAC.

the average queue length increases. With more packets entering the transit buffer, the total successful transmission probability *PS* also increases (since more packets have the opportunity of occupying PLC and VLC channels). Accordingly, the expected QoI $E[Q_s]$ increases. It can be observed that the proposed analytical model correctly captures the performance of the HPVC MAC despite the fact that a larger buffer size slightly increases the deviation between simulation and analysis results (a phenomenon caused by increased system jitter [56, Chapter 4]).

Here is an example of expected QoI $E[Q_s]$ for HPVC MAC ($K \in [2, 10]$). The simulation results of $E[Q_s]$ vary from 3.549 to 4.001 using RA CS; from 3.614 to 4.030 using TA CS; from 3.428 to 3.925 using CA CS.

The numerical analysis results of $E[Q_s]$ vary from 3.673 to 4.114 using RA CS; from 3.733 to 4.136 using TA CS; from 3.560 to 4.059 using CA CS.

5.4. The impact of required minimum SNR

It should be stressed that the required minimum SNR ζ_p&ζ_v would alter the performance of HPVC MAC as well. Here the specifying parameters are set as $N = 40$, $K = 2$, $\lambda = 20$, $\lambda_{th} = 18$ (i.e., $CE = 0.9$), $Q_s = 10$, $\zeta_p \in [0\text{ dB}, 6\text{ dB}]$ and $\zeta_v \in [4\text{ dB}, 10\text{ dB}]$, we can see the Goodput *Gp* and expected QoI $E[Q_s]$ decrease with the increase of ζ_p&ζ_v (shown in Fig. 11). The reason is that as ζ_p and ζ_v increase, the outage probabilities $F_\gamma(\zeta_p)$ and $G_\gamma(\zeta_v)$ increase (they are two monotone increasing functions). In other words, the packets are easier to be received in outage. As a consequence, the values of *Gp* and $E[Q_s]$ are reduced (verified by Eqs.(46) and (47)).

Table 4
The results of HPVC MAC under RA CS and TA CS.

RA CS	$\frac{1}{E[U]}$	P_{OF}	$E[\mathcal{Q}]$
Sim	0.0314 s	0.1949	0.7003
Ana	0.0302 s	0.1852	0.6772
TA CS	$\frac{1}{E[U]}$	P_{OF}	$E[\mathcal{Q}]$
Sim	0.0277 s	0.1652	0.6283
Ana	0.0269 s	0.1586	0.6118

Since ζ_p&ζ_v cannot influence the values of P_{PLC} and P_{VLC} under RA CS and TA CS (unlike CA CS, these two strategies do not rely on the channel state), $P_\Phi|\Phi \in \{p, v\}$ under RA CS and TA CS would be unchanged (described in Section 4.1). Accordingly, the results of average MAC service time $\frac{1}{E[U]}$, average queue length $E[\mathcal{Q}]$ and overflow probability P_{OF} for HPVC MAC using RA CS and TA CS (please see Table 4) should not be affected as well (this conclusion can be verified by the contents of Section 4.2.3 and **Appendix A**). As shown in Fig. 12, the performance of $\frac{1}{E[U]}$, $E[\mathcal{Q}]$ and P_{OF} for HPVC MAC using CA CS decreases with the increase of ζ_p&ζ_v. That is because although the increased ζ_p&ζ_v decreases the successful reception probability of a packet (for using CA CS), it may lead to superior channel selection result, and accordingly increase the overall medium service efficiency.

Here is an example of overflow probability P_{OF} for HPVC MAC using CA CS ($\zeta_p \in [0\text{ dB}, 6\text{ dB}]$, $\zeta_v \in [4\text{ dB}, 10\text{ dB}]$). The simulation results of P_{OF} varies from 0.1786 to 0.1530; while the numerical analysis results varies from 0.1880 to 0.1591.

Remark 7. In our paper, the ACK frames used in HPVC MAC have fixed lengths (that is because the ACK frames of IEEE 1901 and IEEE 802.15.7 are generally hardware-based [27,28], which cannot be arbitrarily modified). If we further assume that the length of ACK frame sent by CP

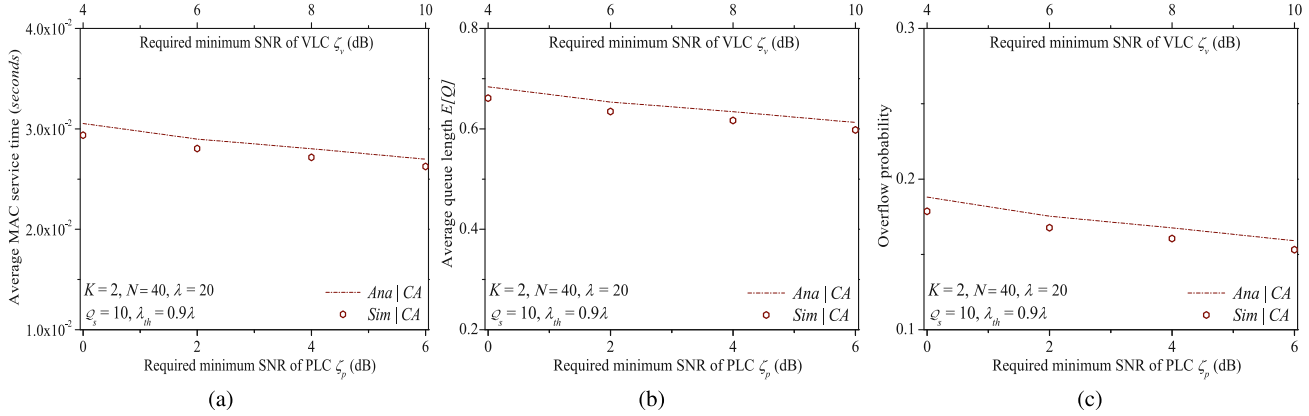

Fig. 12. Performance of $1/E[U]$, $E[\mathcal{Q}]$ and P_{OF} for HPVC MAC using CA CS.

station is based on transmission states (i.e., the length of ACK frame corresponding to successful transmission is different from that corresponding to reception in outage), the performance of average MAC service time $\frac{1}{E[U]}$, average queue length $E[\mathcal{Q}]$ and overflow probability P_{OF} for HPVC MAC will be affected by ζ_p&ζ_v no matter using RA CS or TA CS.

6. Conclusion

In this paper, a MAC protocol based on CSMA/CA for HPVC network is designed (HPVC MAC). Firstly, the PLC and VLC channel resources are efficiently utilized by developing random allocation, traffic-aware and channel-aware-based Channel Selection (CS) strategies, then the CSMA/CA mechanism of HPVC MAC is implemented on the base of combining existing IEEE 1901 and 802.15.7 standards. The performance of HPVC MAC is characterized through typical metrics including Goodput, MAC service time, overflow probability, queue length and expected QoI. Some interesting insights are thereafter drawn from simulation results: (1) Different CS strategies obviously result in different performance of HPVC MAC. That is to say modifying the CS strategy can further enhance the performance of HPVC MAC. (2) The proposed MAC protocol is affected by the specifying parameters of HPVC networks, e.g., network size, traffic rate, required minimum SNR and etc. Hence, adjusting parameters is an available solution for optimizing HPVC MAC. (3) It is difficult to guarantee that all metrics of the HPVC MAC have the best performance under the same parameter settings; for example, a lower overflow probability may be accompanied by a poorer Goodput performance.

In addition to proposing the HPVC MAC protocol, we construct a joint analytical model for evaluating the HPVC MAC that integrates the effects of PHY and MAC layer settings, CS strategies, and actual environmental parameters. To ensure the mathematical rigour, we further prove the proposed model is solvable. Comparing the simulation results with numerical results derived by this model, we reach the conclusion that despite using the simplified Queueing model, our analytical model is still enough accurate (the average error rate is 4.62%). To the best of our knowledge, this should be the first study to design a MAC protocol for HPVC networks and establish a corresponding analysis framework. Our work provides a significant paradigm for exploring the MAC layer of HPVC networks, which is valuable for realizing the target of cooperative communication.

This work can be extended from the following research directions: (1) Analyzing the energy consumption for HPVC networks; (2) Considering the impacts of PHY layer retransmission protocols on HPVC MAC; (3) Optimizing the performance of HPVC networks.

Declaration of competing interest

The work described has not been submitted elsewhere for publication, in whole or in part. No conflict of interest exits in the submission of this manuscript, and manuscript is approved by all authors for publication.

Acknowledgment

The author would like to thank the editor, anonymous reviewers and Prof. Yan Jiao Chen for helpful comments that have improved the quality of the paper. This work was supported by the National Natural Science Foundation of China (No.61772386), National Key Research and Development Project (No.2018YFB1305001) and Fundamental Research Funds for the Central Universities (No.KJ02072021-0119).

Appendix A. Derivation process of $E[U_p]$ (using PLC channel)

Assuming the sensor station (using PLC channel) makes a transmission at backoff stage i, then the average spent time $T_p(j)$ at backoff stage $j|j<i$ can be divided as three parts:

(a) If the initial selected backoff counter is no more than d_j+1, the average spent time $T_p^1(j)$ is given by

$$T_p^1(j)=\frac{1}{Q_j}\cdot\sum_{q=1}^{d_j+1}\sum_{x=0}^{q-1}[t_c+(q-x-1)\sigma+xt_b]p_p^x(1-p_p)^{q-1-x} \tag{A.1}$$

where t_c denotes the time duration due to a collision at PLC channel, t_b the busy time duration. Based on the frame setting of IEEE 1901 [27], t_c is denoted as

$$t_c=EIFS \tag{A.2}$$

where *EIFS* represents the extended inter-frame space.

t_b is derived as

$$t_b=\frac{(N_p-1)\tau_p\cdot(1-\tau_p)^{N_p-2}}{p_p}\cdot t_s+\left(1-\frac{(N_p-1)\tau_p\cdot(1-\tau_p)^{N_p-2}}{p_p}\right)\cdot t_c \tag{A.3}$$

where t_s is the time for a successful transmission at PLC MAC layer (without considering whether the packet is received in outage), and it can be computed as [27].

$$t_s=2PRS+PR+D+RIFS+ACK+CIFS+\Delta \tag{A.4}$$

In Eq.A.4, *PRS*, *PR*, *RIFS*, *CIFS*, *ACK* and *D* denote the priority tone slot, preamble, response inter-frame space, contention inter-frame space, acknowledgment frame of 1901 and frame duration of data packet in PLC channel, respectively.

(b) If the initial selected backoff counter is larger than $d_j + 1$ and the deferral counter mechanism of 1901 protocol is not triggered, the average spent time $T_p^2(j)$ is obtained as

$$T_p^2(j) = \frac{1}{Q_j} \cdot \sum_{q=d_j+2}^{Q_j} \sum_{x=0}^{d_j} [t_c + (q-x-1)\sigma + xt_b] C_{q-1}^{x} p_p^x (1-p_p)^{q-1-x} \tag{A.5}$$

(c) If the deferral counter mechanism of 1901 protocol is triggered at stage j, the average spent time $T_p^3(j)$ is represented as

$$T_p^3(j) = \frac{1}{Q_j} \cdot \sum_{q=d_j+2}^{Q_j} \sum_{x=d_j+1}^{q} [t_b + (x-d_j-1)\sigma + d_j t_b] C_{x-1}^{d_j} p_p^{d_j} (1-p_p)^{x-1-d_j} \tag{A.6}$$

Accordingly, we can write $T_p(j)$ as

$$T_p(j) = T_p^1(j) + T_p^2(j) + T_p^3(j) \tag{A.7}$$

Since the transmission happens at backoff stage i, the average spent time $T_p(i)$ at stage i can be divided into $T_p^1(i)$ (the initial backoff counter is no more than $d_i + 1$) and $T_p^2(i)$ (the initial backoff counter is larger than $d_i + 1$ without triggering the deferral counter mechanism).

Thus, we can express $T_p(i)$ as the following equation

$$T_p(i) = T_p^1(i) + T_p^2(i) = \frac{1}{Q_i} \left\{ \sum_{q=1}^{d_i+1} \sum_{x=0}^{q-1} [t_s + (q-x-1)\sigma + xt_b] p_p^x (1-p_p)^{q-1-x} + \sum_{q=d_i+2}^{Q_i} \sum_{x=0}^{d_i} [t_s + (q-x-1)\sigma + xt_b] C_{q-1}^{x} p_p^x (1-p_p)^{q-1-x} \right\} \tag{A.8}$$

Now the MAC service time $\mathbb{T}_p(i)$ that a transmission occurs at backoff stage i (using PLC channel) can be respectively written as

$$\mathbb{T}_p(i) = \left[\sum_{j=1}^{i-1} T_p(j) \cdot p_p^{i-j} + T_p(i) \right]; \quad i \in [1, m-1] \tag{A.9}$$

$$\mathbb{T}_p(m) = \left[\sum_{j=1}^{m-1} T_p(j) \cdot p_p^{m-j} \right] + \sum_{y=1}^{+\infty} \left[\sum_{j=1}^{m-1} T_p(j) \cdot p_p^{m-j} + T_p(m) \right] p_p^y + T_p(m) \tag{A.10}$$

Accordingly, the average MAC service time $\mathbb{T}_p$ that a sensor station makes a transmission using PLC channel can be derived as

$$\mathbb{T}_p = \sum_{i=1}^{m} \mathbb{T}_p(i) \cdot (1-p_p) \tag{A.11}$$

$E[U_p]$ is finally represented as

$$E[U_p] = \frac{1}{\mathbb{T}_p} \tag{A.12}$$

Appendix B. Derivation process of $E[Q_s]$'s upper bound

Let $E[Q_s] = f(\tau_v, \tau_p)$ (i.e., a binary function), then we take the partial derivative for $f(\tau_v, \tau_p)$:

$$\frac{\partial f(\tau_v, \tau_p)}{\partial \tau_v} = Q_s \cdot (1 - G_\gamma(\zeta_v)) \cdot N_v (1 - N_v \tau_v) \cdot (1-\tau_v)^{N_v - 2} \tag{B.1}$$

$$\frac{\partial f(\tau_v, \tau_p)}{\partial \tau_p} = Q_s \cdot (1 - F_\gamma(\zeta_p)) \cdot N_p (1 - N_p \tau_p) \cdot (1-\tau_p)^{N_v - 2} \tag{B.2}$$

If $\frac{\partial f(\tau_v, \tau_p)}{\partial \tau_v} = 0$ and $\frac{\partial f(\tau_v, \tau_p)}{\partial \tau_p} = 0$, we have the optimal values of τ_v and τ_p, i.e.,

$$\begin{cases} \tau_v = \dfrac{1}{N_v} \\ \tau_p = \dfrac{1}{N_p} \end{cases} \tag{B.3}$$

Hence, the upper bound performance of expected QoI $[E[Q_s]]^+$ is developed as

$$[E[Q_s]]^+ = Q_s \cdot \left[\left(1 - G_\gamma(\zeta_v)\right) \cdot \left(1 - \frac{1}{N_v}\right)^{N_v - 1} + \left(1 - F_\gamma(\zeta_p)\right) \cdot \left(1 - \frac{1}{N_p}\right)^{N_p - 1} \right] \tag{B.4}$$

For $N \to +\infty$, $[E[Q_s]]^+$ can be further expressed as

$$\lim_{N\to+\infty}[E[Q_s]]^+ = Q_s[(1-F_\gamma(\zeta_p))+(1-G_\gamma(\zeta_v))]exp(-1) \tag{B.5}$$

References

[1] N. Gershenfeld, R. Krikorian, D. Cohen, The internet of things, Sci. Am. 291 (4) (2004) 76.
[2] J. Yang, B. Ai, I. You, M. Imran, L. Wang, K. Guan, et al., Ultra-reliable communications for industrial internet of things: design considerations and channel modeling, IEEE Netw. 33 (4) (2019) 104–111.
[3] M. Ke, Z. Gao, Y. Wu, X. Gao, K.K. Wong, Massive access in cell-free massive mimo-based internet of things: cloud computing and edge computing paradigms, IEEE J. Sel. Area. Commun. 39 (3) (2021) 756–772.
[4] A. Mellit, S. Kalogirou, Artificial intelligence and internet of things to improve efficacy of diagnosis and remote sensing of solar photovoltaic systems: challenges, recommendations and future directions, Renew. Sustain. Energy Rev. 143 (2021) 110889.
[5] M.A. Amirabadi, V.T. Vakili, Performance analysis of a novel hybrid FSO/RF communication system, IET Optoelectron. 14 (2) (2020) 66–74.
[6] X. Li, R. Zhang, L. Hanzo, Cooperative load balancing in hybrid Visible Light communications and WIFI, IEEE Trans. Commun. 63 (4) (2015) 1319–1329.
[7] W. Si, D. Starobinski, M. Laifenfeld, A robust load balancing and routing protocol for intra-car hybrid wired/wireless networks, IEEE Trans. Mobile Comput. 18 (2) (2019) 250–263.
[8] A. Kumar, S.K. Ghorai, Ber performance analysis of OFDM-based integrated PLC and MIMO-VLC system, IET Optoelectron. 14 (5) (2020) 242–251.
[9] M. Kashef, M. Abdallah, N. Al-Dhahir, Transmit power optimization for a hybrid PLC/VLC/RF communication system, IEEE Transac. Green Commun. Netw. 2 (1) (2018) 234–245.
[10] A.R. Ndjiongue, H.C. Ferreira, S. Jian, C. Ling, Hybrid PLC-VLC channel model and spectral estimation using a nonparametric approach, Transac. Energ. Telecommun. Technol. 28 (12) (2017) 28.
[11] M. Hao, L. Lampe, S. Hranilovic, Hybrid visible light and power line communication for indoor multiuser downlink, IEEE/OSA J. Opt. Commun. Netw. 9 (8) (2017) 635–647.
[12] M. Jani, P. Garg, A. Gupta, Performance analysis of a co-operative PLC/VLC system with multiple access points for indoor broadcasting, AEU Int. J. Electron. Commun. 103 (2019) 64–73.
[13] M. Jani, P. Garg, A. Gupta, On the performance of a cooperative PLC-VLC indoor broadcasting system consisting of mobile user nodes for IoT networks, IEEE Trans. Broadcast. 67 (1) (2020) 289–298.
[14] M. Jani, P. Garg, A. Gupta, Performance analysis of a mixed cooperative PLC-VLC system for indoor communication systems, IEEE Syst. J. 14 (1) (2020) 469–476.
[15] W. Gheth, K.M. Rabie, B. Adebisi, M. Ijaz, G. Harris, Performance analysis of integrated power-line/visible-light communication systems with AF relaying, in: IEEE Global Communications Conference, United Arab Emirates, Abu Dhabi, 9-13 Dec. 2018.
[16] S. Feng, T. Bai, L. Hanzo, Joint Power Allocation for the Multi-User NOMA-Downlink in a Power-Line-Fed VLC Network, IEEE Transactions on Vehicular Technology, 2019, pp. 5185–5190.
[17] A. Naz, B. Baig, H.M. Asif, Non Orthogonal Multiple Access (NOMA) for broadband communication in smart grids using VLC and PLC - ScienceDirect, Optik 188 (2019) 162–171.
[18] IEEE 1901 HD-PLC (high definition power line communication). www.hd-plc.org. (Accessed February 2018).
[19] C. Cano, A. Pittolo, D. Malone, L. Lampe, A.M. Tonello, A.G. Babak, State of the art in power line communications: from the applications to the medium, IEEE J. Sel. Area. Commun. 34 (7) (2016) 1935–1952.
[20] H. Liu, X. Pu, Y. Chen, J. Yang, J. Chen, User-centric access scheme based on interference management for indoor VLC-WIFI heterogeneous networks, IEEE Photon. J. 12 (4) (2020) 7903712.
[21] V. Fernandes, H.V. Poor, M.V. Ribeiro, Dedicated energy harvesting in concatenated hybrid PLC-wireless systems, IEEE Trans. Wireless Commun. 19 (6) (2020) 3839–3853.
[22] T. Nogueira, G.R. Colen, V. Fernandes, M.V. Ribeiro, Statistical modeling of magnitudes of Brazilian in-home PLC and hybrid PLC-wireless channels, Phys. Commun. 39 (2020) 101014.
[23] Q. Li, T. Cao, W. Sun, W. Li, J. Li, An optimal uplink scheduling in heterogeneous PLC and LTE communication for delay-aware Smart Grid applications, Mobile Network. Appl. 4 (2021) 1–14.
[24] A. Jovicic, J. Li, T.J. Richardson, Methods and Apparatus for Efficient Joint Power Line and Visible Light Communication, 2015. Patent No. US9166683.
[25] T.K. Tran, H. Yahoui, N. Siauve, N. Nguyen-Quang, D. Genon-Catalot, Construct and control a PV-based independent public LED street lighting system with an efficient battery management system based on the power line communication, in: Proceedings of IEEE Second International Conference on DC Microgrids (ICDCM), 2017, pp. 497–501.
[26] H. Khalid, F. Waris, et al., Design of an integrated power line communication (PLC)-visible light communication (VLC) system for data communication, Laser Eng. 40 (2018) 107–125.
[27] IEEE standard for broadband over power line networks: medium access control and physical layer specifications, IEEE Std 1901-2010 10 (2) (2010) 1–1589.
[28] IEEE standard for local and metropolitan area networks–Part 15.7: short-range optical wireless communications, IEEE Std 802.15.7-2018 (Revision of IEEE Std 802.15.7-2011) (2019) 1–407.
[29] A. Mathur, Y. Ai, M. Cheffena, M.R. Bhatnagar, Performance of hybrid ARQ over power line communications channels, in: Proceedings of IEEE 91st Vehicular Technology Conference, Belgium, May 2020, pp. 1–6.
[30] G. Artale, A. Cataliotti, V. Cosentino, et al., A new low cost power line communication solution for smart grid monitoring and management, IEEE Instrum. Meas. Mag. 21 (2) (2018) 29–33.
[31] Homeplug alliance. www.homeplug.org. (Accessed 12 June 2016).
[32] K. Patil, K.D. Turck, D. Fiems, A two-queue model for optimising the value of information in energy-harvesting sensor networks, Perform. Eval 119 (2018) 27–42.
[33] D. Pengfei, Q. Yang, H. Qingsu, K. Kwak, Energy-aware quality of information maximization for wireless sensor networks, IET Commun. 10 (17) (2016) 2281–2289.
[34] M.H. Jung, M.Y. Chung, T.J. Lee, MAC throughput analysis of HomePlug1.0, IEEE Commun. Lett. 9 (2) (2005) 184–186.
[35] C. Vlachou, A. Banchs, J. Herzen, P. Thiran, Performance analysis of mac for power-line communications, in: SIGMETRICS, USA, 2014, pp. 585–586.
[36] C. Vlachou, A. Banchs, J. Herzen, P. Thiran, Analyzing and boosting the performance of power-line communication networks, in: Proceedings of the 10th International on Conference on Emerging Networking Experiments and Technologies, CoNEXT, 2014, pp. 1–12.
[37] C. Vlachou, A. Banchs, J. Herzen, P. Thiran, On the MAC for power-line communications: modeling assumptions and performance tradeoffs, Semiotica 2007 (166) (2014) 97–104.
[38] C. Vlachou, A. Banchs, P. Salvador, Analysis and enhancement of CSMA/CA with deferral in power-line communications, IEEE J. Sel. Area. Commun. 34 (7) (2016) 1978–1991.
[39] C. Vlachou, A. Banchs, J. Herzen, P. Thiran, How CSMA/CA with deferral affects performance and dynamics in power-line communications, IEEE/ACM Trans. Netw. 25 (1) (2017) 250–263.
[40] C. Cano, D. Malone, On efficiency and validity of previous Homeplug MAC performance analysis, Comput. Network. 83 (2016) 118–135.
[41] S. Hao, H.Y. Zhang, From homogeneous to heterogeneous: an analytical model for IEEE 1901 power line communication networks in unsaturated conditions, IEICE Trans. Commun. E102-B (8) (2019) 1636–1648.
[42] S. Hao, H.Y. Zhang, Theoretical modeling for performance analysis of IEEE 1901 power-line communication networks in the multi-hop environment, J. Supercomput. 76 (2020) 2715–2747.
[43] N.T. Le, S. Choi, Y.M. Jang, Cooperative MAC protocol for LED-ID systems, in: Proceedings of ICT Convergence (ICTC), Seoul, Korea (South), 2011, pp. 144–150.
[44] A. Musa, M.D. Baba, H. Mansor, Performance analysis of the IEEE 802.15.7 CSMA/CA algorithm based on Discrete Time Markov chain (DTMC), in: IEEE Malaysia International Conference on Communications, Kuala Lumpur, Malaysia, Nov. 2013, pp. 385–389.
[45] S.K. Nobar, K.A. Mehr, J.M. Niya, Comprehensive performance analysis of IEEE 802.15.7 CSMA/CA mechanism for saturated traffic, IEEE/OSA J. Opt. Commun. Netw. 7 (2) (2015) 62–73.
[46] K.A. Mehr, S.K. Nobar, J.M. Niya, IEEE 802.15.7 MAC under unsaturated traffic: performance analysis and queue modeling, IEEE/OSA J. Opt. Commun. Netw. 7 (9) (2015) 875–884.
[47] N.T. Dang, V.V. Mai, A PHY/MAC cross-layer analysis for IEEE 802.15.7 uplink visible local area network, IEEE Photon. J. 11 (3) (2019) 1–17.
[48] S. Hao, H.Y. Zhang, An energy harvesting modified MAC protocol for power-line communication systems using RF energy transfer: design and analysis, IEICE Trans. Commun. E103-B (10) (2020) 1086–1100.
[49] S. Hao, H.Y. Zhang, MAC performance analysis for reliable power-line communication networks with ARQ scheme, Sensors 21 (1) (2020) 196.
[50] S. Hao, H.Y. Zhang, A cross-layered theoretical model of IEEE 1901 power-line communication networks considering retransmission protocols, IEEE Access 9 (2021) 28805–28821.
[51] I.S. Gradshteyn, I.M. Ryzhikand, A. Jeffrey, Table of Integrals, Series, and Products, Academic Press, 1980.
[52] G. Bolch, S. Greiner, H.D. Meer, K.S. Trivedi, Queuing Networks and Markov Chains, Wiley, Hoboken, NJ, USA, 1998.
[53] Iglehart, L. Donald, Weak convergence in queueing theory, Adv. Appl. Probab. 5 (1973) 570–594, 03.
[54] R.W. Hamming, Numerical Methods for Scientists and Engineers, Dover Publications, St. Mineola, NY, 1973.
[55] M. Dupac, B.M. Dan, Engineering Applications: Analytical and Numerical Calculation with MATLAB, John Wiley and Sons Ltd, USA, 2021.
[56] K.J. Astrom, Introduction to Stochastic Control Theory, Academic Press, USA, 1970.